KIAS-Q25016

Causal Bounds on EFTs with anomalies with a Pseudoscalar, Photons, and Gravitons

Ziyu Dong[a,1], Jaehoon Jeong[b,2] and Alex Pomarol[c,d,3]

[a] *The Abdus Salam ICTP, Strada Costiera 11, 34135, Trieste, Italy*
[b] *Quantum Universe Center, KIAS, Seoul 02455, Korea*
[c] *IFAE and BIST, Universitat Autònoma de Barcelona, 08193 Bellaterra, Barcelona*
[d] *Departament de Física, Universitat Autònoma de Barcelona, 08193 Bellaterra, Barcelona*

Abstract

Theories with pseudoscalars that couple through anomalies (such as axion models) are of particular phenomenological interest. We carry out a comprehensive analysis of all bounds obtainable from bootstrapping the amplitudes when a pseudoscalar couples to photons and gravitons. This allows us to find new cutoff scales of theories with anomalies that are more restrictive than those obtained from naive perturbative analysis. Our results are especially relevant for holographic models, as the bounds determine the allowed region of the five-dimensional EFTs, for example, by imposing strong bounds on Chern-Simons terms. We also consider modifications of General Relativity in photon–graviton couplings and show that current experiments are sensitive to these effects only if new physics appears at $\sim 10^{-10}$ eV.

Contents

[1]zdong@ictp.it
[2]jeong229@kias.re.kr, jeong229@gmail.com
[3]alex.pomarol@uab.cat

1 Introduction

The S-matrix bootstrap program, which consists of imposing fundamental principles such as unitarity, causality, and crossing symmetry on scattering amplitudes, has proven to be a very powerful tool for constraining Effective Field Theories (EFTs) [1–52]. By relying only on general consistency conditions, this approach has provided robust, model-independent constraints on the (Wilson) coefficients of higher-dimensional operators.

Theories with anomalies are of special interest in this context, as certain higher-dimensional operators, such as those describing the coupling of a Goldstone boson to photons or gravitons, are entirely fixed by symmetry considerations. In such cases, bootstrap techniques can be used to determine new cutoff scales for the theories, which are more stringent than naive perturbative estimates [25, 48]. In the present work, we build upon the analysis of Ref. [48] and undertake a systematic study of all bounds that can be derived from bootstrapping amplitudes involving pseudoscalars, photons, and gravitons.

The inclusion of gravitons plays a central role. The spin-2 nature of the graviton causes scattering amplitudes to grow more rapidly with energy, making the leading Wilson coefficients directly accessible through dispersion relations. Moreover, gravity provides a double-subtracted dispersion relation whose positivity allows one to constrain higher-dimensional operator coefficients as a function of the Newton constant G_N. The price to pay is that dispersion relations must be smeared in order to obtain nontrivial bounds [18, 26, 27]. Nevertheless, the smearing method has already been proven to be very efficient in many processes (see for example [10,28,39,42,44,45,47,49–51]). Alternatively, one could use a time-delay analysis [53], where similar bounds could also be derived [25].

We will show that in theories with anomalies, such as axion models, causality imposes a cutoff scale which lies below that determined by perturbativity. At this cutoff scale, massive states with spin $J \geq 2$ must necessarily appear. In particular, we will derive the bound

$$M_{J\geq 2} \lesssim \sqrt{\frac{c_{4\gamma}}{G_N}\frac{F_\pi^2}{\kappa\kappa_g}}\,, \tag{1.1}$$

where κ (κ_g) is the coupling of the pseudoscalar to photons (gravitons) dictated by anomalies, F_π is the decay constant and $c_{4\gamma}$ is the 4-photon coupling at low-energies, $c_{4\gamma}e^4F_{\mu\nu}^4$. For completeness, we will also study bounds on other non-minimal couplings. For example, we will show that the coupling κ_1 between photons and gravitons, arising from the $R_{\mu\nu\rho\sigma}F^{\mu\nu}F^{\rho\sigma}$ interaction, is related to the presence of $J \geq 3$ states:

$$e^2|\kappa_1| \lesssim \frac{1}{M_{J\geq 3}^2}\,, \tag{1.2}$$

where e is the electric charge.

We will show that our bounds, although derived in four dimensions (4D), can be applied to constrain 5D theories with Chern–Simons terms. They may thus have significant implications for 5D holographic duals of strongly-coupled theories [54]. For example, the Chern–Simons terms can play an important role in holographic duals of hydrodynamical systems at finite temperature and chemical potential [55–64], where sizeable Chern–Simons coefficients have been shown to lead to phase transitions, instabilities, or causality violations [58, 59, 62, 63].

Furthermore, our results can be straightforwardly generalized to theories involving scalar fields instead of pseudoscalars [25], although in that case the relevant couplings are not fixed by anomalies.

The paper is organized as follows. In Sec. 2, we introduce all possible 3-point couplings involving pseudoscalars, photons and gravitons (η, γ, h), and their relation to anomalies. In Sec. 3, we derive the needed dispersion relations and discuss which $2 \to 2$ amplitudes are relevant to bootstrap in order to get bounds on anomalous and non-minimal couplings. In Sec. 4, we explicitly derive the bounds on $\kappa\kappa_g$ and κ_1. In Sec. 5, we discuss the implications of the bounds in axion models, strongly-coupled theories, and 5D (holographic) models, and conclude in Sec. 6. In three Appendices we present technical details on the derivations of the bounds. In Appendix A, we introduce a novel way to derive improved dispersion relations for $t \leftrightarrow u$ symmetric amplitudes. In Appendix B, we list the explicit forms of smeared Wigner d-functions used in the main text. In Appendix C, we discuss all details for the positivity of smeared Wigner d-functions.

2 Three-point interactions involving η, γ, and h

Let us begin by examining all possible on-shell 3-point (3-pt) interactions in theories containing a pseudoscalar η, a photon γ and a graviton h, which will define the EFT $\mathcal{L}_{\rm EFT}(\eta,\gamma,h)$ that we want to bootstrap. We will use the spinor-helicity formalism [65] with the convention that all states are incoming. In this work, we restrict for simplicity to a CP-symmetric EFT.

We first construct the on-shell 3-pt amplitudes characterizing the anomalous couplings of a pseudoscalar (dashed line) to two photons (curly lines) and to two gravitons (double-curly lines). These are given by

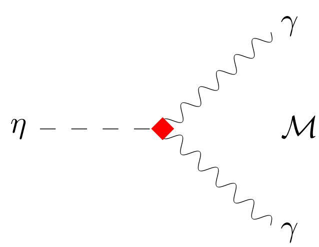

$$\mathcal{M}_{\eta\gamma^+\gamma^+} = \frac{e^2\kappa}{F_\pi}[23]^2$$

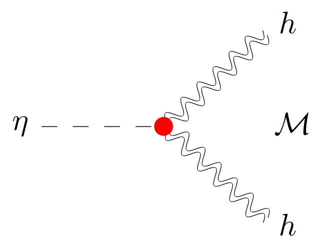

$$\mathcal{M}_{\eta h^+ h^+} = \frac{\kappa_g}{F_\pi M_P^2}[23]^4 \tag{2.1}$$

where M_P denotes the Planck scale, F_π the decay constant of the pseudoscalar η, e the electric coupling, while κ, κ_g are dimensionless anomaly coefficients. The parametrization is chosen such that each graviton contributes a factor of $1/M_P$, each photon a factor of e, and each pseudoscalar a factor of $1/F_\pi$ in the amplitudes. As shown in Eq. (2.1), we will mark with a red diamond (circle) the vertex involving κ (κ_g). The amplitudes in Eq. (2.1) arise in theories with an anomalous $U(1)_\eta$ symmetry, under which $\eta \to \eta + \theta$. They come from the following terms in the Lagrangian:

$$\frac{ie^2\kappa}{F_\pi}\,\eta\,\varepsilon^{\mu\nu\rho\sigma}F_{\mu\nu}F_{\rho\sigma} \quad \text{and} \quad \frac{i\kappa_g}{F_\pi}\,\eta\,\varepsilon^{\mu\nu\rho\sigma}R_{\mu\nu\alpha\beta}R_{\rho\sigma}{}^{\alpha\beta}\,, \tag{2.2}$$

where $F_{\mu\nu}$ and $R_{\mu\nu\rho\sigma}$ are the field strength and Riemann curvature tensors. Therefore κ characterizes the $U(1)_\eta \times U(1)_{\rm EM} \times U(1)_{\rm EM}$ anomaly, while κ_g corresponds to the $U(1)_\eta$-gravitational anomaly.

Additionally, there are 3-pt amplitudes involving non-minimal couplings of a graviton to two photons and three gravitons:

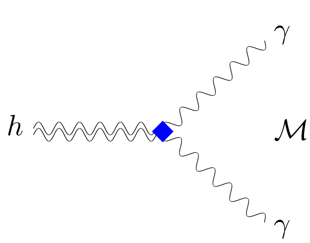

$$\mathcal{M}_{h^+\gamma^+\gamma^+} = \frac{e^2\kappa_1}{M_P}[12]^2[31]^2$$

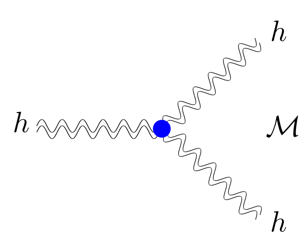

$$\mathcal{M}_{h^+h^+h^+} = \frac{\kappa_3}{M_P^3}[12]^2[23]^2[31]^2 \tag{2.3}$$

where the coefficients κ_1, κ_3 have mass dimension -2. These amplitudes arise respectively from

$h^{\pm}h^{\pm}\gamma^{+}$	Bose symmetry
$h^{+}h^{-}\gamma^{+}$	Factorization consistency
$h^{+}\gamma^{+}\eta$ & $h^{+}\gamma^{-}\eta$	Factorization consistency
$\gamma^{+}\gamma^{+}\gamma^{+}$ & $\gamma^{+}\gamma^{+}\gamma^{-}$	Bose symmetry
$\gamma^{+}\eta\eta$	Bose symmetry
$\eta\eta\eta$	CP symmetry

Table 1: Forbidden 3-pt on-shell interactions involving η, γ, and h.

the following higher-dimensional operators:

$$e^2\kappa_1\, R_{\mu\nu\rho\sigma}F^{\mu\nu}F^{\rho\sigma} \quad \text{and} \quad \kappa_3\, R_{\mu\nu\rho\sigma}R^{\rho\sigma\alpha\beta}R_{\alpha\beta}^{\ \ \ \mu\nu}\,. \tag{2.4}$$

Apart from the 3-pt amplitudes discussed above, the EFT also contains the minimal gravitational couplings of a pseudoscalar, a photon, and a graviton, as described in General Relativity (GR). They correspond to the interactions $h^{\pm}\eta\eta$, $h^{\pm}\gamma^{+}\gamma^{-}$ and $h^{\pm}h^{+}h^{-}$.

Other 3-pt interactions are forbidden for the reasons shown in Table 1. In particular, the amplitudes with two identical particles are antisymmetric under spinor exchange, violating Bose symmetry; CP symmetry excludes the interaction of three pseudoscalars, and the remaining cases do not generate any 4-pt amplitude consistent with factorization [65].

3 Bootstrapping $\mathcal{L}_{\rm EFT}(\eta,\gamma,h)$ from four-point amplitudes

Our goal is to provide an analysis of all possible 4-pt amplitudes involving η, γ, and h that can yield bounds on anomalous and non-minimal couplings, Eq. (2.1) and Eq. (2.3) respectively. We begin by reviewing how analyticity, crossing symmetry, and unitarity impose constraints on the low-energy parameters of scattering amplitudes. We will consider that the UV completions of $\mathcal{L}_{\rm EFT}(\eta,\gamma,h)$ consists of theories with (infinite) weakly-coupled particles, such that 4-pt amplitudes are mediated by the exchange of single states. This makes the analysis less cumbersome. Nevertheless, our results also extend to the case where this assumption is relaxed.[4] Effects of gravity loops have been considered in [49, 50].

3.1 Smeared dispersion relations

Let us consider $2 \to 2$ processes whose amplitudes $\mathcal{M}$ can be expressed as functions of the Mandelstam variables s, t, u. For fixed real $t < 0$, causality ensures that $\mathcal{M}(s,u)$ is analytic throughout the complex s-plane, except along the real axis. In the case of amplitudes mediated by tree-level

[4]For example, new physics appearing in the amplitudes at the loop level were considered in [66], where it was shown that causal bounds persist.

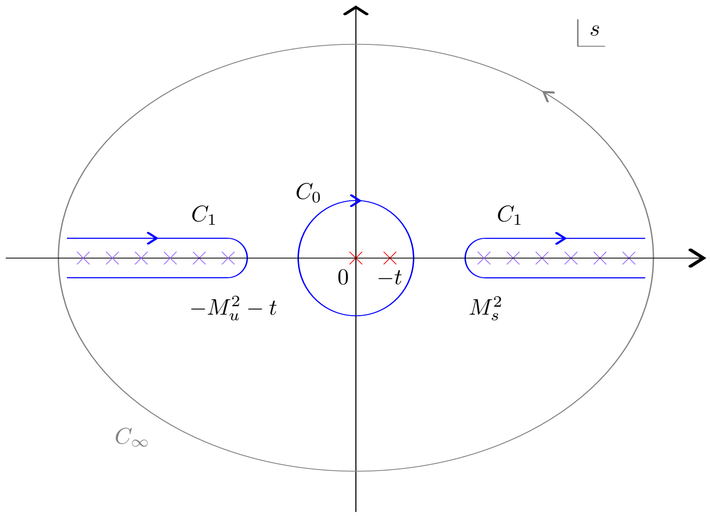

Figure 1: Contours in the complex s-plane used to obtain dispersion relations. The red crosses mark the poles from massless exchanges in the amplitudes at low-energies, while the purple crosses indicate poles associated with the heavy states of the UV completion.

exchange, the singularities reduce to simple poles only on the real s-axis, as depicted in Fig. 1 where M_s (M_u) corresponds to the mass of the first UV state in the s-channel (u-channel).

We can derived what is called a k-subtracted dispersion relation in the following way. Let us consider the function

$$\frac{\mathcal{M}(s,u)}{s^{1+k-l}(s+t)^l}\,, \tag{3.1}$$

where k and $l \leq k$ are nonnegative integers to be specified later. By Cauchy's theorem we have that the integration of this function along the C_∞ contour of Fig. 1, $\int_{C_\infty} \mathcal{M}/(s^{1+k-l}(s+t)^l) \equiv 2iR_\infty$, is equivalent, by deforming the contour, to the integral along C_0 and C_1 of Fig. 1. The contour integral along C_1 picks up the non-analytical part of the amplitude that is related to its imaginary part. This provides the following relation:

$$\frac{1}{2i}\oint_{C_0} ds' \frac{\mathcal{M}(s',-s'-t)}{s'^{1+k-l}(s'+t)^l} = \int_{M_s^2}^{\infty} ds' \frac{\mathrm{Im}\mathcal{M}(s',-t-s')}{s'^{1+k-l}(s'+t)^l} + (-1)^k \int_{M_u^2}^{\infty} ds' \frac{\mathrm{Im}\mathcal{M}(-t-s',s')}{(s'+t)^{1+k-l}s'^l} + R_\infty(t)\,. \tag{3.2}$$

We can expand $\mathrm{Im}\mathcal{M}$ in partial-waves [67] using the Wigner d-functions. In particular,

$$\begin{aligned} \mathrm{Im}\mathcal{M}_{\lambda_1,\lambda_2,\lambda_3,\lambda_4}(s,-t-s) &= \sum_J (2J+1)\rho_J(s) d^J_{\lambda_{12},\lambda_{43}}\left(1+\frac{2t}{s}\right), \\ \text{with} \quad (2J+1)\rho_J(s) &= \pi \sum_i g_{\lambda_1\lambda_2,i}\, g_{\lambda_3\lambda_4,i}\; m_i^2 \delta(s-m_i^2)\, \delta_{J,J_i}\,, \end{aligned} \tag{3.3}$$

where $\lambda_{ab} = \lambda_a - \lambda_b$ with λ_a being the helicity of the external state a, and the couplings $g^2_{\lambda_a\lambda_b,i}$ appear from the residues of the s-channel poles. The corresponding u-channel expression follows from

	Bound derived			No bound derived		
Ref. [48]	$h^+h^+h^-h^-$	κ_g^2 & κ_3^2	$k=3$	$h^+h^+h^+h^+$	κ_g^2 & κ_3	$k=2$
	$h^+h^-\eta\eta$	κ_g^2	$k=2$	$\eta\eta\eta h^+$	κ_g	$k=2$
	$h^+h^+h^-\eta$	κ_g & $\kappa_g\kappa_3$	$k=2$			
This work	$h^+h^+\gamma^-\gamma^-$	$\kappa\kappa_g$ & $\kappa_1\kappa_3$	$k=2$	$\gamma^+\gamma^-h^+\eta$	κ_g & $\kappa\kappa_1$	$k=2$
	$h^+h^+\gamma^+\gamma^+$	$\kappa\kappa_g$ & κ_1	$k=2$			
	$h^+h^-\gamma^+\gamma^+$	κ_1	$k=2$	$\gamma^+\gamma^+h^-\eta$	$\kappa_1\kappa_g$	$k=2$
	$h^+h^-\gamma^+\gamma^-$	κ_1^2	$k=3$			

Table 2: External states, η, $\gamma^\pm$ and $h^\pm$, of an amplitude whose k-subtracted dispersion relation involves the anomaly coefficients (κ, κ_g) or non-minimal couplings (κ_1, κ_3). The first line shows the amplitudes studied in Ref. [48], while the second are those discussed in the present work. We also indicate whether a bound on the 3-pt coefficients can be obtained. Amplitudes not shown do not involve the 3-pt couplings of Eq. (2.1) and Eq. (2.3).

Eq. (3.3) with the replacement $s \to u$ together with $\lambda_2 \leftrightarrow \lambda_4$. We also introduce, for convenience, the "high-energy average"

$$\langle (...) \rangle = \frac{1}{\pi}\int_{M_{s,u}^2}^{\infty} \frac{dm^2}{m^2} \sum_J (2J+1)\rho^J(m^2)(...)\,. \tag{3.4}$$

With all this, Eq. (3.2) can be recast in the following way:

$$\frac{1}{2\pi i}\oint_{C_0} ds' \frac{\mathcal{M}(s',-s'-t)}{s'^{1+k-l}(s'+t)^l} = \left\langle \frac{d^J_{\lambda_{12},\lambda_{43}}(1+2t/m^2)}{m^{2(k-l)}(m^2+t)^l} \right\rangle + (-1)^k \left\langle \frac{d^J_{\lambda_{14},\lambda_{23}}(1+2t/m^2)}{(m^2+t)^{1+k-l} m^{2l-2}} \right\rangle + R_\infty(t)\,. \tag{3.5}$$

The dependence on R_∞ makes the above relation no very useful. In principle, the Froissart-Martin bound [68,69] tells us that for $k \geq 2$, $R_\infty \to 0$. Nevertheless, we are dealing with γ and h as internal massless states, and therefore the Froissart-Martin bound is not directly applicable. To get rid of R_∞ in Eq. (3.5), we will integrate this relation over t with a proper "smearing function" $A(t)$ to be discussed later. The reason for this smearing is twofold. On one hand, we avoid singularities $1/t$ due to the graviton pole in the amplitudes. On the other hand, it can be proven [26] that $\int_{-|t|_{\max}}^0 dt\, A(t)\, R_\infty(t) \to 0$ for $k \geq 2$. In this way, we get the smeared dispersion relation:

$$\frac{1}{2\pi i}\int_{-|t|_{\max}}^0 dt\, A(t) \oint_{C_0} ds' \frac{\mathcal{M}(s',-s'-t)}{s'^{1+k-l}(s'+t)^l} = \int_{-|t|_{\max}}^0 dt\, A(t) \left[\left\langle \frac{d^J_{\lambda_{12},\lambda_{43}}(1+\frac{2t}{m^2})}{m^{2(k-l)}(m^2+t)^l} \right\rangle + (-1)^k \left\langle \frac{d^J_{\lambda_{14},\lambda_{23}}(1+\frac{2t}{m^2})}{(m^2+t)^{1+k-l} m^{2l-2}} \right\rangle \right]. \tag{3.6}$$

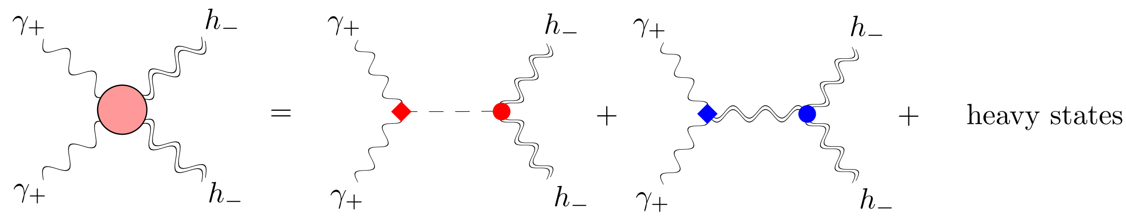

Figure 2: Contributions to the process $\gamma^+\gamma^+ \to h^+h^+$. All helicities are indicated in the all-incoming convention. The red diamond and circle represent resprectively the anomaly couplings κ and κ_g, while the blue diamond and circle correspond to the non-minimal couplings κ_1 and κ_3.

3.2 Relevant four-point amplitudes with η, γ and h

Armed with the smeared dispersion relations Eq. (3.6), we aim to obtain all possible bounds on the couplings of Eq. (2.1) and Eq. (2.3) using all amplitudes involving as external states η, γ and h. In Table 2 we present a summary of the amplitudes whose k-subtracted dispersion relation involves any of the couplings of Eq. (2.1) and Eq. (2.3). The table also specifies whether a bound can be obtained or not. A brief comment is in order.

Amplitudes involving only η and h as external states were already studied in Refs. [25,48], and bounds on κ_g and κ_3 were obtained there. Therefore we will not discuss them here any longer.[5]

We will center in processes involving γ. In particular, we will consider $\gamma^+\gamma^+ \to h^+h^+$ that is sensitive to $\kappa\kappa_g$ and $\kappa_1\kappa_3$, as shown in Fig. 2. From this process we will be able to derive a bound on $\kappa\kappa_g$. Similarly, the process $\gamma^+\gamma^+ \to h^-h^-$ also involve $\kappa\kappa_g$ and a bound will also be derived, although it will be more model dependent.

Additionally, we will consider the process $\gamma^+h^+ \to \gamma^-h^+$, shown in Fig. 4, which is sensitive to κ_1 thanks to the γ and h exchange, that will allow to bound this coupling. The elastic process $\gamma^+h^- \to \gamma^+h^-$ could also be used to bound κ_1, although it leads to a similar bound, and we will not derive it here.

In Table 2 we also show other 4-pt amplitudes from which, although their dispersion relations involve anomalous or non-minimal couplings, we have not been able to derive any bound. This is because we always encounter infinitely many Wilson coefficients in these cases. Other amplitudes not shown in Table 2 do not involve the 3-pt couplings of Eq. (2.1) and Eq. (2.3).

4 Bootstrapping $\kappa\kappa_g$ and κ_1

4.1 $\gamma^+\gamma^+ \to h^+h^+$

At low-energies the amplitude for the scattering $\gamma^+\gamma^+ \to h^+h^+$ is given by (see Fig. 2)

$$\mathcal{M}_{\gamma^+\gamma^+h^-h^-} = s^3\left(\frac{e^2\kappa\kappa_g}{F_\pi^2 M_P^2 s} + \frac{e^2\kappa_1\kappa_3 tu}{M_P^4 s} + \cdots\right), \tag{4.1}$$

[5]The presence of γ as an internal state does not afffect the dispersion relations of these amplitudes.

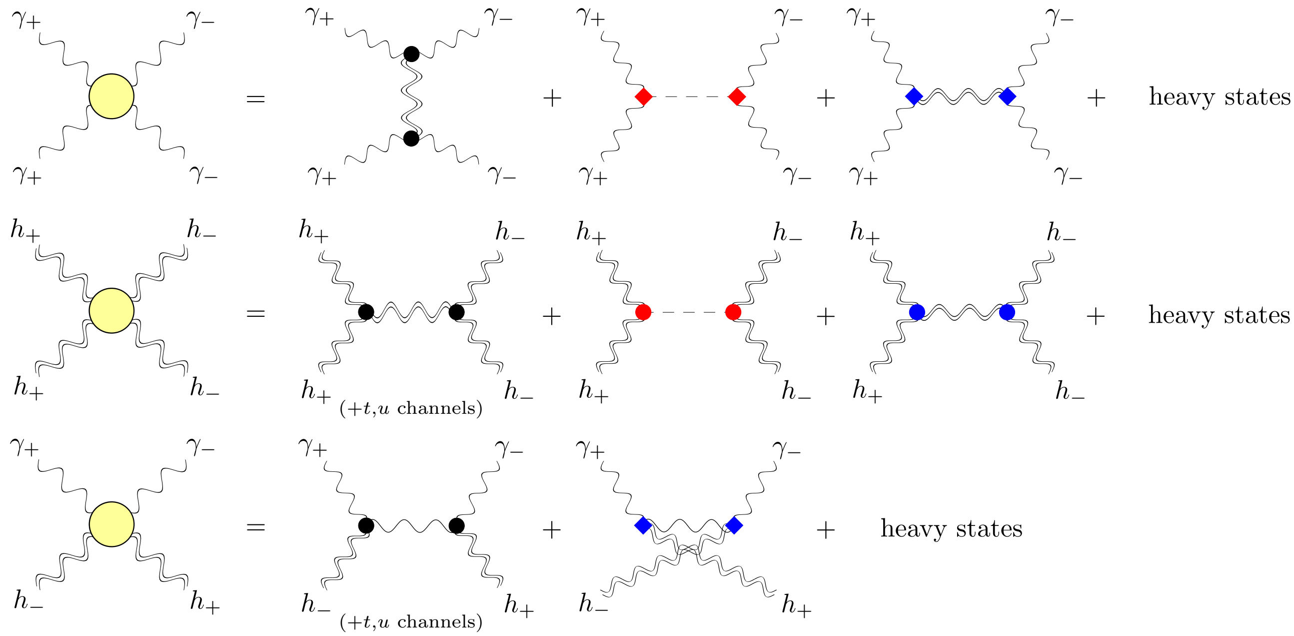

Figure 3: Contributions to the three elastic processes $\gamma^+\gamma^+ \to \gamma^+\gamma^+$, $h^+h^+ \to h^+h^+$, and $\gamma^+h^- \to \gamma^+h^-$. The red and blue markers correspond to the couplings introduced in Fig. 2. The black circle represents the gravitational minimal coupling.

where $\kappa\kappa_g$ appears from the s-channel η exchange, while $\kappa_1\kappa_3$ from the h exchange.[6] Here the symbol $\cdots$ corresponds to contact-term polynomials in s, t, u.

Because Eq. (4.1) is an inelastic amplitude, for which positivity bounds do not hold, we must relate it to elastic amplitudes: $\gamma^+\gamma^+ \to \gamma^+\gamma^+$, $h^+h^+ \to h^+h^+$, and $\gamma^+h^- \to \gamma^+h^-$, shown in Fig. 3. At low-energies these are given by

$$\mathcal{M}_{\gamma^+\gamma^+\gamma^-\gamma^-} = s^2\left(\frac{1}{M_P^2 w} + \frac{e^4\kappa_1^2 w}{M_P^2} - \frac{e^4\kappa^2}{F_\pi^2 s} + e^4 c_{4\gamma} + \cdots\right), \quad w \equiv \frac{tu}{s}, \tag{4.2}$$

$$\mathcal{M}_{h^+h^+h^-h^-} = s^4\left(\frac{1}{M_P^2 stu} - \frac{\kappa_g^2}{F_\pi^2 M_P^2 s} + \frac{\kappa_3^2 tu}{M_P^6 s} + \cdots\right), \tag{4.3}$$

$$\mathcal{M}_{\gamma^+h^-\gamma^-h^+} = -su^3\left(\frac{1}{M_P^2 stu} - \frac{e^4\kappa_1^2}{M_P^2 u} + \cdots\right). \tag{4.4}$$

For the four-photon amplitude we have introduced a new variable, $w = tu/s$. The reason is the following. $k = 2$ dispersion relations at fixed t involve infinitely many low-energy Wilson coefficients from contact terms, and are therefore impractical. Nevertheless, taking the amplitude at fixed w, we will be able to obtain dispersion relations that only depend on one Wilson coefficient, $c_{4\gamma}$ (see Appendix. A for details). That is, in the case of $t \leftrightarrow u$ symmetry, the variable substitution of w can directly obtain the improved dispersion relation in [18, 26].

Let us derive $k = 2$ dispersion relations for these four processes. Using Eq. (3.5) with $l = 0$ and

[6] We omit a little-group helicity phase, which has no impact on analyticity.

Eq. (4.1) for the inelastic process, we get

$$\frac{e^2\kappa\kappa_g}{F_\pi^2 M_P^2} - \frac{e^2\kappa_1\kappa_3 t^2}{M_P^4} = \left\langle \frac{d^J_{0,0}\left(1+\frac{2t}{m^2}\right)}{m^4} \right\rangle^{g_{\gamma^+\gamma^+}}_{g_{h^-h^-}} + \left\langle \frac{m^2(-1)^J d^J_{3,3}\left(1+\frac{2t}{m^2}\right)}{(m^2+t)^3} \right\rangle^{g_{\gamma^+h^-}}_{g_{\gamma^+h^-}} + R_\infty(t)\,. \tag{4.5}$$

For the elastic processes, we have using Eq. (A.5) with Eq. (4.2):

$$\frac{1}{M_P^2 w} + \frac{e^4\kappa_1^2 w}{M_P^2} + e^4 c_{4\gamma} = \left\langle \frac{d^J_{0,0}\left(\sqrt{1-\frac{4w}{m^2}}\right)}{m^4} \right\rangle^{g_{\gamma^+\gamma^+}}_{g_{\gamma^-\gamma^-}} + \left\langle \frac{d^J_{2,2}\left(\frac{m^2-w}{m^2+w}\right)}{m^8}(m^2+2w)(m^2+w) \right\rangle^{g_{\gamma^+\gamma^-}}_{g_{\gamma^-\gamma^+}} + R_\infty(t)\,, \tag{4.6}$$

and from Eq. (3.5) with $l = 0$ and 2, together with Eq. (4.3) and Eq. (4.4) respectively, we get

$$-\frac{1}{M_P^2 t} = \left\langle \frac{d^J_{0,0}\left(1+\frac{2t}{m^2}\right)}{m^4} \right\rangle^{g_{h^+h^+}}_{g_{h^-h^-}} + \left\langle \frac{m^2 d^J_{4,4}\left(1+\frac{2t}{m^2}\right)}{(m^2+t)^3} \right\rangle^{g_{h^+h^-}}_{g_{h^-h^+}} + R_\infty(t), \tag{4.7}$$

$$-\frac{1}{M_P^2 t} = \left\langle \frac{d^J_{3,3}\left(1+\frac{2t}{m^2}\right)}{(m^2+t)^2} \right\rangle^{g_{\gamma^+h^-}}_{g_{\gamma^-h^+}} + \left\langle \frac{m^2 d^J_{1,1}\left(1+\frac{2t}{m^2}\right)}{m^2(m^2+t)} \right\rangle^{g_{\gamma^+h^+}}_{g_{\gamma^-h^-}} + R_\infty(t). \tag{4.8}$$

The super- and subscripts denote the couplings appearing in the residues of the s- and u-channel poles, respectively. As we commented before, smearing over these relations with smearing functions, $A(t), B(t), ...$, we can get rid of R_∞ and obtain

$$\int_{-|t|_{\max}}^{0} dt\, A(t)\left(\frac{e^2\kappa\kappa_g}{F_\pi^2 M_P^2} - \frac{e^2\kappa_1\kappa_3 t^2}{M_P^4}\right) = \sum_i^{\text{s-ch}} A_s(m_i, J_i)\, g_{\gamma^+\gamma^+,i}\, g_{h^-h^-,i}, + \sum_i^{\text{u-ch}} A_u(m_i, J_i)\, g^2_{\gamma^+h^-,i}, \tag{4.9}$$

$$\int_0^{w_{\max}} dw\, B(w)\left(\frac{1}{M_P^2 w} + \frac{e^4\kappa_1^2 w}{M_P^2} + e^4 c_{4\gamma}\right) = \sum_i^{\text{s-ch}} B_s(m_i, J_i)\, |g_{\gamma^+\gamma^+,i}|^2 + \sum_i^{\text{u-ch}} B_u(m_i, J_i)\, |g_{\gamma^+\gamma^-,i}|^2, \tag{4.10}$$

$$\int_{-|t|_{\max}}^{0} dt\, C(t)\frac{-1}{M_P^2 t} = \sum_i^{\text{s-ch}} C_s(m_i, J_i)\, |g_{h^+h^+,i}|^2 + \sum_i^{\text{u-ch}} C_u(m_i, J_i)\, |g_{h^+h^-,i}|^2, \tag{4.11}$$

$$\int_{-|t|_{\max}}^{0} dt\, D(t)\frac{-1}{M_P^2 t} = \sum_i^{\text{s-ch}} D_s(m_i, J_i)\, |g_{\gamma^+h^-,i}|^2 + \sum_i^{\text{u-ch}} D_u(m_i, J_i)\, |g_{\gamma^+h^+,i}|^2, \tag{4.12}$$

where the explicit forms of smeared Wigner d-functions $A_{s,u}, B_{s,u}, C_{s,u}$, and $D_{s,u}$ are presented in Appendix. B.

Toward deriving the bounds, the first condition on the smeared Wigner d-functions is their positivity in terms of all allowed values of m_i and J_i. This allows to derive the following simplified inequalities for the dispersion relations of the elastic processes:

$$B_{s,u}(m_i,J_i)\geq 0 \;\;\Rightarrow\;\; \int_0^{w_{\max}} dw\, B(w)\left(\frac{1}{M_P^2 w}+\frac{e^4\kappa_1^2 w}{M_P^2}+e^4 c_{4\gamma}\right) \geq \sum_i^{\text{s-ch}} B_s(m_i,J_i)\,|g_{\gamma^+\gamma^+,i}|^2, \tag{4.13}$$

$$C_{s,u}(m_i,J_i)\geq 0 \;\;\Rightarrow\;\; \int_{-|t|_{\max}}^{0} dt\, C(t)\frac{-1}{M_P^2 t} \geq \sum_i^{\text{s-ch}} C_s(m_i,J_i)\,|g_{h^+h^+,i}|^2, \tag{4.14}$$

$$D_{s,u}(m_i,J_i)\geq 0 \;\;\Rightarrow\;\; \int_{-|t|_{\max}}^{0} dt\, D(t)\frac{-1}{M_P^2 t} \geq \sum_i^{\text{s-ch}} D_s(m_i,J_i)\,|g_{\gamma^+h^-,i}|^2. \tag{4.15}$$

Secondly, in order to bound the inelastic process Eq. (4.9), we demand the conditions

$$|A_s(m_i,J_i)|\leq\sqrt{B_s(m_i,J_i)C_s(m_i,J_i)}\;,\qquad |A_u(m_i,J_i)|\leq D_s(m_i,J_i)\,, \tag{4.16}$$

that respectively lead to

$$\sum_i^{\text{s-ch}} |A_s(m_i,J_i)\, g_{\gamma^+\gamma^+,i}\, g_{h^-h^-,i}| \leq \sum_i^{\text{s-ch}} |\sqrt{B_s(m_i,J_i)}\, g_{\gamma^+\gamma^+,i}|\,|\sqrt{C_s(m_i,J_i)}\, g_{h^-h^-,i}|, \tag{4.17}$$

$$\sum_i^{\text{u-ch}} |A_u(m_i,J_i)\, g^2_{\gamma^+h^-,i}| \leq \sum_i^{\text{s-ch}} D_s(m_i,J_i)\,|g_{\gamma^+h^-,i}|^2\,. \tag{4.18}$$

Notice that the smeared Wigner d-functions $A_{s,u}$ are not required to be positive. In order to relate the RHS of Eq. (4.17) to the RHS of Eq. (4.13) and Eq. (4.14), we use the Cauchy–Schwarz inequality

$$\begin{aligned}&\sum_i^{\text{s-ch}} |\sqrt{B_s(m_i,J_i)}\, g_{\gamma^+\gamma^+,i}||\sqrt{C_s(m_i,J_i)}\, g_{h^-h^-,i}|\\ &\leq \sqrt{\left(\sum_i^{\text{s-ch}} B_s(m_i,J_i)|g_{\gamma^+\gamma^+,i}|^2\right)\left(\sum_i^{\text{s-ch}} C_s(m_i,J_i)|g_{h^+h^+,i}|^2\right)}\,.\end{aligned} \tag{4.19}$$

Collecting all the formulas discussed above, we can construct the following relation:

$$\begin{aligned}&\left|\sum_i^{\text{s-ch}} A_s(m_i,J_i)\, g_{\gamma^+\gamma^+,i}\, g_{h^-h^-,i},+\sum_i^{\text{u-ch}} A_u(m_i,J_i)\, g^2_{\gamma^+h^-,i}\right|\\ &\leq \sqrt{\left(\sum_i^{\text{s-ch}} B_s(m_i,J_i)|g_{\gamma^+\gamma^+,i}|^2\right)\left(\sum_i^{\text{s-ch}} C_s(m_i,J_i)|g_{h^+h^+,i}|^2\right)}+\sum_{J,i}^{\text{s-ch}} D_s(m_i,J_i)\,|g_{\gamma^+h^-,i}|^2,\end{aligned} \tag{4.20}$$

leading to the inequality between the low-energy sides,

$$\left| \int_{-|t|_{\max}}^{0} dt\, A(t) \left(\frac{e^2 \kappa \kappa_g}{F_\pi^2 M_P^2} - \frac{e^2 \kappa_1 \kappa_3 t^2}{M_P^4} \right) \right|$$
$$\leq \sqrt{ \left\{ \int_0^{w_{\max}} dw\, B(w) \left(\frac{1}{M_P^2 w} + \frac{e^4 \kappa_1^2 w}{M_P^2} + e^4 c_{4\gamma} \right) \right\} \left\{ \int_{-|t|_{\max}}^{0} dt\, C(t) \frac{-1}{M_P^2 t} \right\} } + \int_{-|t|_{\max}}^{0} dt\, D(t) \frac{-1}{M_P^2 t}\,, \tag{4.21}$$

that provides a bound on the anomalous couplings. This bound simplifies when neglecting sub-leading $1/M_P$ terms:

$$\left| \frac{\kappa \kappa_g}{F_\pi^2 M_P^2} \int_{-|t|_{\max}}^{0} dt\, A(t) \right| \leq \sqrt{ \frac{c_{4\gamma}}{M_P^2} \int_0^{w_{\max}} dw\, B(w) \int_{-|t|_{\max}}^{0} dt\, C(t) \frac{-1}{t} }\,. \tag{4.22}$$

The smearing functions must be chosen to satisfy all the conditions mentioned above. A choice of these functions is (see Appendix C for a detailed discussion)

$$A(t) = C(t) = (1 - \sqrt{-t/|t|_{\max}})^5, \tag{4.23}$$
$$B(w) = 4\,(1 - \sqrt{w/w_{\max}})^5, \tag{4.24}$$
$$D(t) = 1.1\, J_0\Big(9\sqrt{-t/|t|_{\max}}\Big)\, (1 - \sqrt{-t/|t|_{\max}})^5, \tag{4.25}$$

where $J_0(x)$ is the Bessel function of the first kind. We take $w_{\max} = |t|_{\max}/4$ to satisfy the inequality in Eq. (4.17).[7] The smearing functions are chosen to satisfy all positivity conditions when $|t|_{\max}$ is smaller than the mass of the lightest heavy state appearing among the three elastic processes. The value of $|t|_{\max}$ plays a crucial role, since the LHS of the bound Eq. (4.22) depends linearly on $\sqrt{|t|_{\max}}$, as can be easily deduced on dimensional grounds. Therefore the larger the value of $|t|_{\max}$, the stronger the bound. Nevertheless, $|t|_{\max}$ cannot exceed the mass of the lightest spin $J \geq 2$ UV state, denoted by $M_{J\geq 2}$, otherwise we lose the positivity of the functions $B_{s,u}, C_{s,u}$ and $D_{s,u}$ (see Appendix C). For this reason, we take

$$|t|_{\max} = M_{J\geq 2}^2\,. \tag{4.26}$$

We will later discuss a particular case where $M_{J\geq 2}$ corresponds to the mass of a $J = 2$ state, which couples to $\gamma^+\gamma^+$ and h^-h^-, and can be exchanged in the processes $\gamma^+\gamma^+ \to \gamma^+\gamma^+$ and $h^+h^+ \to h^+h^+$. This is consistent with causality bounds for higher-spin particles in the large N_c limit [70–73].

[7] The factor 4 in the smearing function was introduced such that the integrals on the high-energy side yield the overall factor $|t|_{\max}$, rather than $|t|_{\max}/4$.

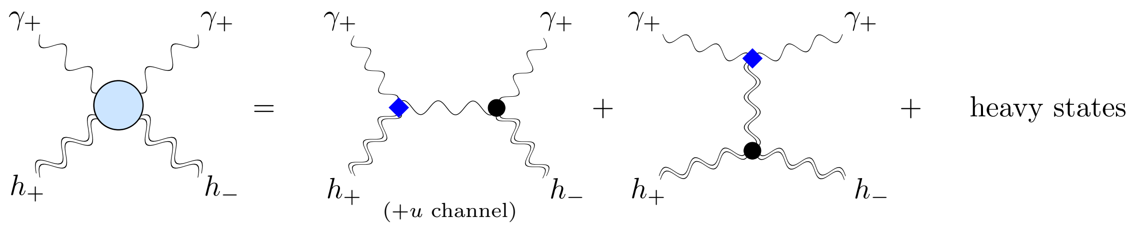

Figure 4: Contributions to the process $\gamma^+ h^+ \to \gamma^- h^+$.

Plugging Eqs. (4.23)–(4.25) and Eq. (4.26) into Eq. (4.22), we get the bound

$$M_{J\geq 2}\frac{|\kappa\kappa_g|}{F_\pi^2 M_P} \lesssim 1.4\sqrt{c_{4\gamma}}\ln^{\frac{1}{2}}\left(\frac{M_{J\geq 2}}{M_{\rm IR}}\right), \tag{4.27}$$

where we have had to introduce the IR cutoff $M_{\rm IR}$ to regularize the logarithmically divergent integral $\int dt\, C(t)/t$. This requirement is a well-known feature of 4D gravity, also manifest in constraints from time delays in the eikonal limit [53] (and the time delay experienced by photons is positive not only at tree level but also at one-loop order).

4.2 $\gamma^+\gamma^+ \to h^- h^-$

In addition to the bound in Eq. (4.27), we can derive an alternative bound on $\kappa\kappa_g$ from the process $\gamma^+\gamma^+ \to h^- h^-$, which amplitude at low-energy, written in terms of the variable w, is given by

$$\mathcal{M}_{\gamma^+\gamma^+h^+h^+} = s\left(\frac{e^2\kappa\kappa_g\, s^2}{F_\pi^2 M_P^2\, s} + \frac{e^2\kappa_1\, s^2}{M_P^2\, w} + \frac{e^2 b_{2,0}\, sw}{M_P^2} + \cdots\right), \tag{4.28}$$

where the first term arises from the η exchange in the s-channel, the second one is for the γ exchange in the t- and u-channel, and $b_{2,0}$ is a Wilson coefficient.

Following the procedure outlined in Sec. 4.1, we get the bound

$$M_{J\geq 2}\left|\frac{\kappa\kappa_g}{F_\pi^2 M_P} + \frac{b_{2,0}M_{J\geq 2}^2}{8M_P}\right| \lesssim 1.4\sqrt{c_{4\gamma}}\ln^{\frac{1}{2}}\left(\frac{M_{J\geq 2}}{M_{\rm IR}}\right), \tag{4.29}$$

that is similar to Eq. (4.27) but contains the additional contribution from $b_{2,0}$.

4.3 $\gamma^+ h^+ \to \gamma^- h^+$

Having established the bounds on $\kappa\kappa_g$, we also derive a bound on the non-minimal coupling κ_1. For this purpose we use the process $\gamma^+ h^+ \to \gamma^- h^+$ whose low-energy amplitude is given by

$$\mathcal{M}_{\gamma^+h^+\gamma^+h^-} = s^2u^2t\left(\frac{e^2\kappa_1}{M_P^2 stu} + \cdots\right), \tag{4.30}$$

where κ_1 appears due to the γ exchange in the s- and u-channels, and h exchange in the t-channel –see Fig. 4. The $s \leftrightarrow u$ symmetric property of the amplitude leads to the following simple form of the dispersion relation with $k = 2$ and $l = 1$ or 2:

$$\frac{e^2\kappa_1}{M_P^2} = \left\langle \frac{(2m^2+t)d^J_{3,1}(1+2t/m^2)}{m^2(m^2+t)^2} \right\rangle^{g_{\gamma^+h^+}}_{g_{\gamma^+h^-}} + R_\infty(t)\,. \tag{4.31}$$

To bound κ_1, we need to compare this to the elastic $\gamma^+h^- \to \gamma^+h^-$, whose contributions are shown at the bottom of Fig. 3 and its dispersion relation is given in Eq. (4.8).

Next, we integrate over the dispersion relations Eqs. (4.31) and (4.8) with some arbitrary smearing functions, $E(t)$ and $F(t)$, respectively:

$$\int_{-|t|_{\max}}^{0} dt\, E(t)\frac{e^2\kappa_1}{M_P^2} = \sum_i^{\text{s-ch}} E_s(m_i, J_i)\, g_{\gamma^+h^+,i}\, g_{\gamma^+h^-,i}, \tag{4.32}$$

$$\int_{-|t|_{\max}}^{0} dt\, F(t)\frac{-1}{M_P^2 t} = \sum_i^{\text{s-ch}} F_s(m_i, J_i)\, |g_{\gamma^+h^-,i}|^2 + \sum_i^{\text{u-ch}} F_u(m_i, J_i)\, |g_{\gamma^+h^+,i}|^2, \tag{4.33}$$

where in Eq. (4.32) we have combined the s- and u-channels using the $s \leftrightarrow u$ symmetry. The explicit forms of E_s and $F_{s,u}$ are presented in Appendix B. As in the procedure for bounding $\kappa\kappa_g$ in Sec. 4.1, the smeared Wigner d-function E_s for the process $\gamma^+h^+ \to \gamma^-h^+$ can be either positive or negative depending on i. With this fact in mind, we impose the following conditions on E_s and $F_{s,u}$:

$$|E_s(m_i, J_i)| \le \sqrt{F_s(m_i, J_i)F_u(m_i, J_i)} \quad \text{and} \quad F_s(m_i, J_i), F_u(m_i, J_i) \ge 0\,, \tag{4.34}$$

that lead to the inequality

$$\sum_i^{\text{s-ch}} |E_s(m_i, J_i)\, g_{\gamma^+h^+,i}\, g_{\gamma^+h^-,i}| \le \sum_i^{\text{s-ch}} |\sqrt{F_s(m_i, J_i)}\, g_{\gamma^+h^-,i}|\, |\sqrt{F_u(m_i, J_i)}\, g_{\gamma^+h^+,i}|\,. \tag{4.35}$$

This inequality remains valid even without the absolute value bars on the LHS. Due to angular momentum conservation, the summation on the RHS must start from $J = 3$, as indicated by the s-ch symbol. Using the Cauchy–Schwarz inequality,

$$\begin{aligned} &\sum_i^{\text{s-ch}} |\sqrt{F_s(m_i, J_i)}\, g_{\gamma^+h^-,i}||\sqrt{F_u(m_i, J_i)}\, g_{\gamma^+h^+,i}| \\ &\le \sqrt{\left(\sum_i^{\text{s-ch}} F_s(m_i, J_i)|g_{\gamma^+h^-,i}|^2\right)\left(\sum_i^{\text{u-ch}} F_u(m_i, J_i)|g_{\gamma^+h^+,i}|^2\right)}, \end{aligned} \tag{4.36}$$

in Eq. (4.35), we get

$$\left|\sum_i^{\text{s-ch}} E_s(m_i,J_i)\, g_{\gamma^+h^+,i}\, g_{\gamma^+h^-,i}\right| \le \sqrt{\frac{1}{2}\left(\sum_i^{\text{s-ch}} F_s(m_i,J_i)\,|g_{\gamma^+h^-,i}|^2 + \sum_i^{\text{u-ch}} F_u(m_i,J_i)\,|g_{\gamma^+h^+,i}|^2\right)^2}\,. \tag{4.37}$$

This, together with Eqs. (4.32) and (4.33), leads to

$$\left|\frac{e^2\kappa_1}{M_P^2}\int_{-|t|_{\max}}^0 dt\,E(t)\right| \le \frac{1}{\sqrt{2}M_P^2}\int_{-|t|_{\max}}^0 dt\,F(t)\frac{-1}{t}, \tag{4.38}$$

implying the linear $|t|_{\max}$ dependence of the bound.

One choice of the smearing functions satisfying the conditions in Eq. (4.34) is given by[8]

$$E(t) = (-t/|t|_{\max})^{5/8}(1-\sqrt{-t/|t|_{\max}})^5, \tag{4.39}$$

$$F(t) = J_0(9\sqrt{-t/|t|_{\max}})(1-\sqrt{-t/|t|_{\max}})^5\,. \tag{4.40}$$

As discussed in Sec. 4.1, we must take the largest possible value for $|t|_{\max}$ without violating the positivity of $F_{s,u}$. This corresponds to (see Appendix C for details)

$$|t|_{\max} = M_{J\ge 3}^2, \tag{4.41}$$

which is the mass of the lightest spin $J \ge 3$ UV states. In the particular case where this UV state has $J = 3$, and couples to γ^+h^+ and γ^-h^+, this is the first massive UV state encountered in the processes $\gamma^+h^+ \to \gamma^+h^+$ and $\gamma^-h^+ \to \gamma^-h^+$.

Plugging Eqs. (4.39) and (4.40) into Eq. (4.38) with (4.41) we obtain the bound

$$e^2|\kappa_1|M_{J\ge 3}^2 \lesssim 226\ln\left(\frac{M_{J\ge 3}}{M_{\text{IR}}}\right), \tag{4.42}$$

where the IR cutoff M_{IR} is required to regulate the logarithmic divergence in $\int dtF(t)/t$.

4.4 $\gamma^+h^- \to \gamma^+h^-$

The elastic scattering $\gamma^+h^- \to \gamma^+h^-$, whose EFT amplitude is given in Eq. (4.4), can solely yield the same type of bound as Eq. (4.42). As shown in Table 2, the appearance of κ_1^2 in the dispersion relation at $k = 3$ allows us to bound it by comparing it with the dispersion relation at $k = 2$. This procedure is the same as that used to bound κ_g from the elastic scattering $h^+h^+ \to h^+h^+$ in Ref. [48]. We leave the explicit computation to the reader, as the full procedure has already been presented in Ref. [48].

[8]For the function $E(t)$ the overall factor $(-t/|t|_{\max})^{5/8}$ was chosen to satisfy the condition Eq. (4.35) at large J (see Appendix C.2).

5 Phenomenological implications

There is a large class of models whose spectrum contains a pseudoscalar, a photon and a graviton with the couplings of Eq. (2.1). The most popular examples are axion models, where the axion is a pseudo-Goldstone boson arising from the spontaneous breaking of a $U(1)_{\rm PQ}$ symmetry, which can be identified with η and generically couples to photons and gravitons as in Eq. (2.1). They can either be generated from UV physics or from a mixing of the axion with the QCD π^0 and η'.

In the bound Eq. (4.27), $M_{J\geq 2}$ can be interpreted as the scale at which states with $J \geq 2$ must appear in the theory coupled linearly to $\gamma\gamma$ and hh –see Eq. (4.26)– and therefore corresponds to an upper bound for the cutoff scale of $\mathcal{L}_{\rm EFT}(\eta,\gamma,h)$. We will refer to this cutoff scale as $\Lambda_{\rm caus}$. From Eq. (4.27), taking $M_{\rm IR} = O(M_{J\geq 2})$, the scale $\Lambda_{\rm caus}$ is parametrically given by

$$\Lambda_{\rm caus} \sim M_P \frac{\sqrt{c_{4\gamma}}\, F_\pi^2}{|\kappa\kappa_g|}\,. \tag{5.1}$$

This cutoff scale can be smaller than $\Lambda_{\rm pert}$, the naive perturbative cutoff scale of $\mathcal{L}_{\rm EFT}(\eta,\gamma,h)$ defined as the scale at which loops become of tree-level order. $\Lambda_{\rm pert}$ can be estimated by the energy scale at which the contribution mediated by η to the amplitude of $\gamma\gamma \to hh$ (first term of Eq. (4.1)) becomes $O(1)$. We find

$$\Lambda_{\rm pert} \sim \sqrt{\frac{M_P F_\pi}{e\,(\kappa\kappa_g)^{1/2}}}\,. \tag{5.2}$$

For sufficiently small $c_{4\gamma}$ or e, one finds $\Lambda_{\rm caus}$ smaller than $\Lambda_{\rm pert}$.

Since $c_{4\gamma}$ is expected to be generated by physics at the cutoff, we can assume $c_{4\gamma} \sim 1/\Lambda_{\rm caus}^4$. In this case Eq. (5.1) leads to

$$\Lambda_{\rm caus} \sim \left(\frac{M_P F_\pi^2}{|\kappa\kappa_g|}\right)^{1/3}\,, \tag{5.3}$$

that tells us that for $\kappa\kappa_g \sim 1$ the cutoff scale lies between M_P and F_π.

We can also interpret Eq. (4.27) as a bound on the smallest value of $\gamma\gamma \to \gamma\gamma$ at low-energies. Taking as an example the largest value for the causal cutoff, $\Lambda_{\rm caus} \sim M_P$, one finds

$$c_{4\gamma} \gtrsim \left(\frac{\kappa\kappa_g}{F_\pi^2}\right)^2\,. \tag{5.4}$$

5.1 Strongly-coupled gauge theories

Strongly-coupled gauge theories with N_F fermions and spontaneous breaking of global symmetries, e.g., $U(1)\times U(1) \to U(1)$, contain a light pseudoscalar state, η, in their spectrum.[9]

[9] In theories like QCD this is the chiral symmetry breaking $U(1)_L \times U(1)_R \to U(1)_V$. In this case the axial $U(1)_A$ current $J_A^\mu = \sum_f \bar{f}\gamma^\mu\gamma^5 f$ is not conserved at the quantum level due to the axial anomaly, and η gets a mass of order $m_\eta^2 \sim N_F M^4/F_\pi^2$ [74, 75]. Nevertheless, in the large-N_c limit this mass is suppressed since $F_\pi^2 \sim N_c M^2 \to \infty$ and then $m_\eta^2 \to 0$.

We can estimate the size of the parameters as a function of N_F and N_c, the number of fermions and "colors" respectively, of the gauge group. In the large-N_c limit the scaling of couplings follows the planar expansion [76, 77], and bootstrap bounds on strongly-coupled theories in this limit have been derived recently [29, 30, 34, 35, 37, 38] (see also [70–73]). For the particular case of $SU(N_c)$ gauge theories, with fermions in the fundamental representation, we have

$$\kappa \sim \kappa_g \sim N_c\sqrt{N_F}\ , \quad F_\pi \sim \sqrt{N_c}\ , \quad c_{4\gamma} \sim N_c N_F\ . \tag{5.5}$$

As stated in [48], demanding that loop corrections to the graviton propagator are smaller than tree-level, leads to a bound on the theory around $M_P/N_c \equiv \Lambda_{\rm QG}$. Plugging the relations (5.5) with $M_P = \Lambda_{\rm QG} N_C$ into Eq. (5.1), we get

$$\Lambda_{\rm caus} \sim \Lambda_{\rm QG}\sqrt{\frac{N_c}{N_F}}\ . \tag{5.6}$$

We see that $\Lambda_{\rm caus}$ is larger or of order of $\Lambda_{\rm QG}$ and therefore no meaningful bound can be derived for the $J \geq 2$ states.

Our analysis can be used however to put bounds on 3-pt couplings generated from these models. For example, Eq. (4.42) leads to a bound on κ_1 as a function of the mass of the lightest $J \geq 3$ state that parametrically is given by

$$e^2|\kappa_1| \lesssim \frac{1}{M^2_{J\geq 3}}\ . \tag{5.7}$$

Since κ_1 can be generated from loops of charged fermion, it scales as $\sum_F q_F^2 N_c$, where q_F is the charge of the fermion, and therefore the bound Eq. (5.7) seems very restrictive in the large-N_c limit. Nevertheless, one must take into account that e^2 is also sensitive to $\sum_F q_F^2 N_c$ as fermions affect the photon propagator. In particular, one has

$$\frac{1}{e^2(\mu)} = \frac{1}{e^2(\mu_0)} + \sum_F \frac{q_F^2 N_c}{6\pi^2}\ln \mu_0/\mu\ . \tag{5.8}$$

From Eq. (5.8), we can estimate a lower limit for the gauge coupling at $\mu \lesssim \mu_0$, $e^2 \gtrsim 1/\sum_F q_F^2 N_c$, that used in Eq. (5.7) leads to

$$\frac{|\kappa_1|}{\sum_F q_F^2 N_c} \lesssim \frac{1}{M^2_{J\geq 3}}\ . \tag{5.9}$$

The above bound is specially interesting for strongly-coupled models with an holographic description (see later for details). In these models the $J \geq 3$ states can be parametrically much heavier than the $J < 3$ states, and therefore Eq. (5.9) tells us that κ_1 must be suppressed.

5.2 5D models and holography

Another class of models whose low-energy spectrum consists of η, γ, and h are 5D models with $U(1)_V \times U(1)_A$ gauge invariance. Its Lagrangian can be written as

$$\begin{aligned}\mathcal{L}_5 &= \int d^4x\, dz\, \sqrt{-g}\Big[M_{P5}^3 \mathcal{R} + M_5\Big(V_{MN}^2 + A_{MN}^2 + c_{4V} V_{MN}^4 + \cdots\Big) \\ &\qquad + \kappa_5\, \epsilon_{MNPQR} A^M F^{NP} F^{QR} + \kappa_{g5}\, \epsilon_{MNPQR} A^M \mathcal{R}_B^{NPA} \mathcal{R}_A^{QRB}\Big]\,, \end{aligned} \tag{5.10}$$

where $M, N, ... = \mu, 4$; V_{MN} and A_{MN} are the field-strength tensors of the $U(1)_V$ and $U(1)_A$, while $\mathcal{R}$ and $\mathcal{R}^{MNPQ}$ are respectively the Ricci scalar and Riemann tensor; M_{P5} and $1/M_5$ are respectively the 5D Planck scale and gauge-coupling squared, and κ_5, κ_{g5} are the dimensionless coefficient of the Chern-Simons terms related to $U(1)_A$ anomalies. The Lagrangian Eq. (5.10) is derived as an expansion in fields and derivatives, with $\text{Dim}[A_M]$=$\text{Dim}[V_M] = 1$, and we have only included one term of dimension 8, V_{MN}^4, that will play an important role in our analysis.

We will assume that the extra dimension z is compactified in a segment (orbifold) and will take as boundary conditions $\partial_z V_\mu = 0$ and $A_\mu = 0$ at both boundaries. For the graviton the boundary condition depends on the metric and it is usually referred to as the Israel junction condition [78]. At low-energies, $E \ll 1/L$, the model has the following massless states: V_μ that we identify with the photon, the fifth-component of A_M, A_5 (a pseudoscalar) that we identify with η, and the graviton $h_{\mu\nu}$. The theory also contains massive states, the Kaluza-Klein (KK) modes, for V_μ, A_μ, and $h_{\mu\nu}$. The Chern-Simons terms proportional to κ_5 and κ_{g5} leads respectively to the couplings of Eq. (2.1).

Let us start considering the case in which the 5D space is flat. We then have [79]

$$F_\pi^2 \sim M_5/L\,, \quad M_P^2 \sim M_{P5}^3 L\,. \tag{5.11}$$

In this theory $c_{4\gamma}$ could either be generated from integrating the KK states or from the higher-dimensional operator V_{MN}^4. We find that in flat space there is no coupling of a single KK mode to two massless V_μ (the photon), due to translational invariance in the 5th dimension. Therefore, $c_{4\gamma}$ cannot be generated at tree-level from integrating out the KK modes, and its only contribution arises from c_{4V}, i.e. $c_{4\gamma} \propto c_{4V}$. Given this and Eq. (5.11), we have that the causal bound Eq. (5.1) can be written as

$$\Lambda_{\text{caus}} \sim \frac{\sqrt{M_5^3 M_{P5}^3 c_{4V}}}{\kappa_5 \kappa_{g5}}\,. \tag{5.12}$$

The scale Λ_{caus} corresponds to the mass of the lightest $J \geq 2$ state that couples to $\gamma\gamma$, that could in principle be the lightest KK graviton, of mass $\sim 1/L$. Nevertheless, as we mentioned before, KK gravitons do not couple to $\gamma\gamma$ and therefore Λ_{caus} must be associated to the mass of a new state. Additionally, since c_{4V} is expected to scale with the 5D cutoff scale of the theory, which can

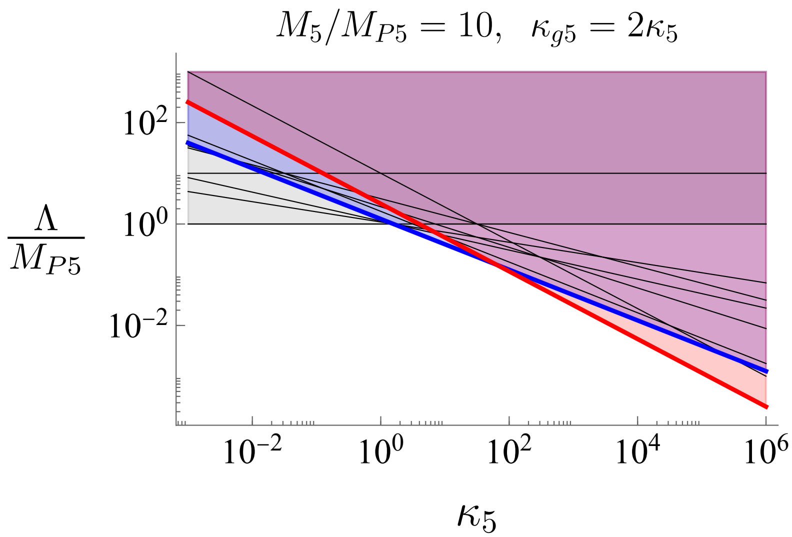

Figure 5: Bounds on the cutoff scale of the 5D model Eq. (5.10). The black lines corresponds to the perturbative bounds Eq. (5.14), while the red (blue) corresponds to the bound from causality Eq. (5.13) (Eq. (5.15)).

be identified with $\Lambda_{\rm caus}$, i.e. $c_{4V} \propto 1/\Lambda^4_{\rm caus}$, we obtain from Eq. (5.12)

$$\Lambda_{\rm caus} \sim \frac{\sqrt{M_5 M_{P5}}}{(\kappa_5 \kappa_{g5})^{1/3}}\,. \tag{5.13}$$

Notice that this bound does not depend on L, so it applies even in the decompactification limit $L \to \infty$.

How Eq. (5.13) compares with other bounds? We can naively get bounds on the cutoff scale of the 5D Lagrangian Eq. (5.10) by demanding that loops are smaller than tree-level effects, i.e. naive dimensional analysis [80]. In particular, we can estimate the cutoff scale $\Lambda_{5\,\rm pert}$ as the scale at which loops in 3-vertices involving V_M and h_{MN} become of order of their tree-level value. This leads to

$$\Lambda_{5\,\rm pert} = {\rm Min}\left\{ M_5, M_{P5}, \frac{M_5}{\kappa_5^{2/3}}, \frac{\sqrt{M_5 M_{P5}}}{\kappa_5^{1/3}}, \sqrt[10]{\frac{M_5 M_{P5}^9}{\kappa_{g5}^2}}, \sqrt[5]{\frac{M_5^2 M_{P5}^3}{\kappa_5 \kappa_{g5}}}, \sqrt[7]{\frac{M_5 M_{P5}^6}{\kappa_{g5}^2}} \right\}. \tag{5.14}$$

Depending on the parameters of the model, we find regions where the causal cutoff Eq. (5.13) is smaller (and therefore more relevant) than the perturbative cutoffs Eq. (5.14). This can be appreciated in Figure 5, where for completeness, we have also included the causal bound obtained in [48]:

$$\Lambda_{\rm caus} \sim \sqrt[4]{\frac{M_5 M_{P5}^3}{\kappa_{g5}^2}}\,. \tag{5.15}$$

It is easy to see for example that the causal upper bound Eq. (5.13) becomes the smallest of all in the limit $\kappa_g \sim \kappa \to \infty$ and $M_5/M_{P5} \sim \kappa^d$ for $0 < d < 2/3$.

Let us now consider the case of warped extra dimensions, for example, the case of an $\rm AdS_5$

metric, $ds^2 = (L/z)^2(\eta_{\mu\nu}dx^\mu dx^\nu - dz^2)$, being L now the AdS curvature radius. We also consider that the extra dimension is limited by two branes, one at $z = 1/\Lambda_{\rm UV}$ (UV-boundary) and another at $z = 1/\Lambda_{\rm IR}$ (IR-boundary) with $\Lambda_{\rm UV} \gg \Lambda_{\rm IR}$ [81]. In holographic language, this setup is dual to a large-N_c CFT with IR breaking [54], which also induces corrections to the graviton propagator [82]. The KK masses are of order $\sim \Lambda_{\rm IR}$ and the scale at which gravity loops are important is given by $\Lambda_{\rm QG} \sim \Lambda_{\rm UV}$. We now have $F_\pi^2 \sim (M_5 L)\Lambda_{\rm IR}^2$ and $M_P^2 \sim (M_{P5}L)^3\Lambda_{\rm UV}^2$. Contrary to the flat case, now $c_{4\gamma}$ can be generated from KK modes. For abelian theories, there is no 3 gauge vertices and the only contribution to $c_{4\gamma}$ comes from the exchange of KK gravitons. One gets the estimate

$$c_{4\gamma} \sim \frac{M_5^2}{M_{P5}^3 L}\frac{1}{\Lambda_{\rm IR}^4}\,. \tag{5.16}$$

Furthermore, now $\Lambda_{\rm caus}$ can be associated with the mass of the lightest KK graviton $\sim \Lambda_{\rm IR}$. Taking all these aspects into account, we derive from Eq. (5.1) the bound

$$\frac{\kappa_5\kappa_{g5}}{(M_5L)^2} \lesssim \frac{\Lambda_{\rm UV}}{\Lambda_{\rm IR}}\,, \tag{5.17}$$

which is naturally interpreted in the dual 4D theory via large-N scaling [54]. Finally, for explicit D3/D7-type holographic realizations, see [83] and [84] for a conformal-collider perspective in holographic CFTs.

The AdS/CFT correspondence relates theories in AdS_5 to 4D strongly-coupled gauge theories in the limit $N_c \to \infty$ and $\lambda \equiv g_{\rm YM}^2 N_c \to \infty$. In these limits, the $J > 2$ states (associated with string excitations) become infinitely heavy, and the light spectrum consists only of states with $J = 0, 1, 2$, as described by Eq. (5.10). The AdS/CFT correspondence dictates

$$M_5 L \sim N_c^r, \quad \kappa_5, \kappa_{g5} \sim N_c^r, \quad \text{and thus} \quad \frac{\kappa_5\kappa_{g5}}{(M_5L)^2} \sim N_c^0\,, \tag{5.18}$$

where $r = 1$ for fermions in the fundamental representation and $r = 2$ for fermions in representations whose number of states grows as N_c^2, such as the symmetric or antisymmetric representations. In both cases, we find that Eq. (5.17) provides an N_c-independent bound on the parameters of the model.

The bound Eq. (5.7) is also particularly interesting for strongly-coupled models in the limit $\lambda \to \infty$. In this regime, in the holographic dual, states with $J \geq 3$ become infinitely heavy, and therefore Eq. (5.7) implies that κ_1 must vanish.

5.3 Astrophysical constraints on the non-minimal coupling κ_1

The $h\gamma\gamma$ non-minimal coupling κ_1 in Eq. (2.4) modifies the photon propagation in curved spacetime, leading to birefringence and helicity-dependent Shapiro delays. The most stringent bound on κ_1 is obtained from the timing of binary pulsar PSR B1534+12 signals that gives $e^2|\kappa_1| \lesssim$

$6\,\mathrm{km}^2$ [85–87], and complementary constraints based on other astrophysical observations can be found in Ref. [88–91].

Astrophysical bounds on κ_1 are typically of order $e^2|\kappa_1|/r_g^2 \lesssim O(1)$, meaning that deviations must remain below the curvature scale set by the gravitational radius r_g, which for black holes corresponds to the horizon radius. For M87* ($r_g \sim 10^9\,\mathrm{km}$), this implies $e^2|\kappa_1| \lesssim 10^{18}\,\mathrm{km}^2$, while for stellar-mass black holes ($r_g \sim 10\,\mathrm{km}$) one finds $e^2|\kappa_1| \lesssim 10^2\,\mathrm{km}^2$.

A $e^2|\kappa_1| \sim 6\,\mathrm{km}^2$, implies, using our bound Eq. (4.42), that there should be new physics at energies

$$\Lambda \sim 8 \times 10^{-11}\,\mathrm{eV}\,. \tag{5.19}$$

This could correspond to new particles with $J \geq 3$ coupled to γh, or, in the case where new physics appears at the loop level, to new states coupled to γ. Such low-mass states should therefore have been observed in other experiments, for example, through their effects on stellar evolution. Our bounds indicate that searches for modifications of GR in binary pulsar timing or similar experiments are not competitive with existing experimental constraints.

6 Conclusion

We have obtained causality bounds by bootstrapping all possible $2 \to 2$ amplitudes EFTs consisting of a pseudoscalar η, a photon γ, and a graviton h, and whose interactions are dictated by $U(1)_\eta$ anomalies, as shown in Eq. (2.1).

To bootstrap amplitudes containing the gravitational t-pole divergence, we integrated the dispersion relation over t or $w = tu/s$ using a weighting function that smears out such divergent contributions. This allowed us to derive, from the process $\gamma^+\gamma^+ \to h^+h^+$, the bound Eq. (4.27) on $\kappa\kappa_g$ as a function of the mass of the $J \geq 2$ states in the EFT's UV completion. For EFTs with anomalies, such as axion models, this bound can be interpreted as a causal UV cutoff of $\mathcal{L}_{\mathrm{EFT}}(\eta, \gamma, h)$ [see Eq. (5.1)]. We have shown that this scale can lie below the perturbative UV cutoff estimated in Eq. (5.2).

In addition, from the process $\gamma^+h^+ \to \gamma^-h^+$, we derived a bound on the non-minimal $h\gamma\gamma$ coupling κ_1, given in Eq. (4.42), as a function of the mass of the lightest $J \geq 3$ UV state.

We further analyzed the implications of our results in strongly-coupled gauge theories and in 5D models with Chern–Simons terms. In the latter case, we showed that the causal cutoff can be smaller than the naive perturbative cutoff scale $\Lambda_{5\mathrm{pert}}$ of Eq. (5.14), especially in the limit $\kappa_g \sim \kappa \to \infty$ and $M_5/M_{P5} \sim \kappa^d$ for $0 < d < 2/3$. We also discussed the implications of these bounds for warped extra-dimensional models, which, thanks to the AdS/CFT correspondence, are related to strongly-coupled gauge theories in the large-N_c and large-λ limits. Our bound Eq. (4.27) provides an N_c-independent constraint on the anomaly coefficients [Eq. (5.17)], while Eq. (5.7) implies that $\kappa_1 \to 0$ as $\lambda \to \infty$.

Finally, we have shown that modifications of General Relativity arising from the photon–graviton coupling κ_1 would require new physics at very low energies, $\sim 10^{-10}$eV, in order to be detectable in current or near-future binary pulsar timing experiments.

Although our bounds were derived in 4D, it would be interesting to obtain these results directly in 5D where log divergences are absent, and analyze their implications for 5D holographic duals of hydrodynamical systems at finite temperature and chemical potential [55–64]. For example, it would be interesting to explore whether violations of our causal bounds are connected to instabilities in these theories. One could also attempt to extend our analysis to theories involving scalar fields, as in [25]. We leave these directions for future work.

Acknowledgments

We thank Yifan Chen and Francesco Sciotti for discussions. AP and ZD have been partly supported by the research grants 2021-SGR-00649 and PID2023-146686NB-C31. JJ was supported by a KIAS Individual Grant (QP090001) through the Quantum Universe Center at the Korea Institute for Advanced Study.

A Improved dispersion relation for $t \leftrightarrow u$ symmetric amplitudes

The $k = 2$ dispersion relation for the amplitude $\gamma^+\gamma^+ \to \gamma^+\gamma^+$ at fixed t involves infinitely many low-energy Wilson coefficients from contact terms. This can be avoided by keeping another variable fixed instead of t in the dispersion relations, as shown in [12, 37, 46, 51, 92] for s-t-u symmetric amplitudes. We present here a similar approach, valid for $t \leftrightarrow u$ symmetric amplitudes, which was *in parallel* elaborated in [93].

We consider the particular case where

$$w \equiv \frac{tu}{s}, \tag{A.1}$$

is taken fixed in a $t \leftrightarrow u$ symmetric amplitude. The expressions for $t(s, w)$ and $u(s, w)$ are given in this case by

$$t = -s\left(\frac{1 - \sqrt{1 - 4w/s}}{2}\right), \quad u = -s\left(\frac{1 + \sqrt{1 - 4w/s}}{2}\right), \tag{A.2}$$

where $w > 0$ in the physical region.[10] For amplitudes symmetric under $t \leftrightarrow u$, the presence of the square roots in Eq. (A.2) does not introduce any non-analyticity, since t and u always appear together in combinations such as $t + u$, tu, etc.[11] For this reason, the non-analytic parts continue

[10] The signs in front of $\sqrt{1 - 4w/s}$ in the expressions of t and u could also be chosen oppositely. In our convention, for $s \to -\infty$, we have $u \to \infty$ while $t \to 0$, indicating nonzero $\mathrm{Im}\,\mathcal{M}$ in the u-channel at $s < 0$. On the other hand, the opposite case leads to nonzero $\mathrm{Im}\,\mathcal{M}$ in the t-channel at $s < 0$.

[11] It indicates that any $t \leftrightarrow u$ symmetric amplitude is independent of the signs in front of $\sqrt{1 - 4w/s}$.

to arise only from the real s axis due to s- and u-channel particle exchanges. They give rise to $\mathrm{Im}\mathcal{M}$ which, as in Sec. 3.1, we expand in partial-waves:

$$\mathrm{Im}\mathcal{M}(s,w) = \sum_{J=\text{even}} (2J+1)\rho^J(s)\, d^J_{\lambda_{12},\lambda_{43}}\left(\sqrt{1-\frac{4w}{s}}\right) \qquad \text{for } s \geq 0\,, \tag{A.3}$$

$$\mathrm{Im}\mathcal{M}(s,w) = \sum_J (2J+1)\rho^J(u)\, d^J_{\lambda_{14},\lambda_{23}}\left(\frac{u-w}{u+w}\right) \qquad \text{for } u \geq 0\,. \tag{A.4}$$

The presence of the squared root in Eq. (A.3) does not pose any problem for $t \leftrightarrow u$ symmetric amplitudes, as it can be understood in the following way. The $t \leftrightarrow u$ symmetry requires that either the incoming or the outgoing particles are the same. Considering the first case, we have $\lambda_{12} = 0$, and consequently that J must be even in Eq. (A.3). In addition, λ_{43} must also be even so, $d^J_{0,\lambda_{43}}$ is an even polynomial in its argument, which guarantees the absence of the square root in Eq. (A.3).

Taking w fixed, we can write the following dispersion relation for $\mathcal{M}(s,w)/s^{1+k}$ using Eq. (A.3) and Eq. (A.4):

$$\frac{1}{2\pi i}\oint_{C_0} ds' \frac{\mathcal{M}(s',w)}{s'^{1+k}} = \left\langle \frac{d^J_{\lambda_{12},\lambda_{43}}\left(\sqrt{1-\frac{4w}{m^2}}\right)}{m^{2k}} \right\rangle + (-1)^k \left\langle \frac{d^J_{\lambda_{14},\lambda_{23}}\left(\frac{m^2-w}{m^2+w}\right)}{m^{4k}} (m^2+2w)(m^2+w)^{k-1} \right\rangle . \tag{A.5}$$

B Explicit expressions of the smeared Wigner d-functions

In this section, we present the explicit formulas for the smeared Wigner d-functions used in the main text.

Those in Eq. (4.9) for $\gamma^+\gamma^+ \to h^+h^+$ are given by

$$A_s(m,J) = \int_{-|t|_{\max}}^0 dt\, A(t) \frac{d^J_{0,0}(1+2t/m^2)}{m^4}, \quad A_u(m,J) = \int_{-|t|_{\max}}^0 dt\, A(t) \frac{m^2(-1)^J d^J_{3,3}(1+2t/m^2)}{(m^2+t)^3}, \tag{B.1}$$

corresponding to the s- and u-channel respectively.

The ones in Eqs. (4.10), (4.11), and (4.12) for $\gamma^+\gamma^+ \to \gamma^+\gamma^+$, $h^+h^+ \to h^+h^+$, and $\gamma^+h^- \to$

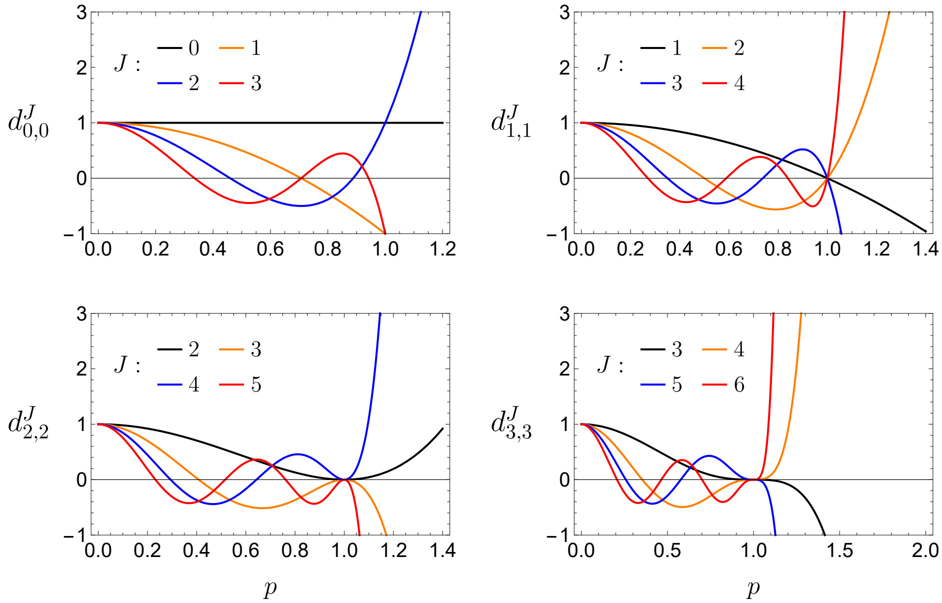

Figure 6: Winger d-functions $d^J_{\lambda,\lambda}(1-2p^2)$.

$\gamma^+ h^-$ are given respectively by

$$B_s(m,J) = \int_0^{w_{\max}} dw\, B(w) \frac{d^J_{0,0}\left(\sqrt{1-\frac{4w}{m^2}}\right)}{m^4}, \tag{B.2}$$

$$B_u(m,J) = \int_0^{w_{\max}} dw\, B(w) \frac{d^J_{2,2}\left(\frac{m^2-w}{m^2+w}\right)}{m^8}(m^2+2w)(m^2+w), \tag{B.3}$$

$$C_s(m,J) = \int_{-|t|_{\max}}^0 dt\, C(t) \frac{d^J_{0,0}\left(1+\frac{2t}{m^2}\right)}{m^4}, \quad C_u(m,J) = \int_{-|t|_{\max}}^0 dt\, C(t) \frac{m^2 d^J_{4,4}\left(1+\frac{2t}{m^2}\right)}{(m^2+t)^3}, \tag{B.4}$$

$$D_s(m,J) = \int_{-|t|_{\max}}^0 dt\, D(t) \frac{d^J_{3,3}\left(1+\frac{2t}{m^2}\right)}{(m^2+t)^2}, \quad D_u(m,J) = \int_{-|t|_{\max}}^0 dt\, D(t) \frac{m^2 d^J_{1,1}\left(1+\frac{2t}{m^2}\right)}{m^2(m^2+t)}. \tag{B.5}$$

In Eq. (4.32) for $\gamma^+ h^+ \to \gamma^- h^+$, we have defined

$$E_s(m,J) = \int_{-|t|_{\max}}^0 dt\, E(t) \frac{(2m^2+t) d^J_{3,1}\left(1+\frac{2t}{m^2}\right)}{m^2(m^2+t)^2}. \tag{B.6}$$

Finally, the functions in Eq. (4.33) for $\gamma^+ h^- \to \gamma^+ h^-$ are

$$F_s(m,J) = \int_{-|t|_{\max}}^0 dt\, F(t) \frac{d^J_{3,3}\left(1+\frac{2t}{m^2}\right)}{(m^2+t)^2}, \quad F_u(m,J) = \int_{-|t|_{\max}}^0 dt\, F(t) \frac{m^2 d^J_{1,1}\left(1+\frac{2t}{m^2}\right)}{m^2(m^2+t)}, \tag{B.7}$$

which are the same as Eq. (B.5), except for the smearing function.

C Positivity of smeared Wigner d-functions

In this section we discuss in detail how to choose the smearing functions and determine $|t|_{\max}$ such that $B_{s,u}(m,J), C_{s,u}(m,J), D_{s,u}(m,J)$ and $F_{s,u}(m,J)$ are positive. All these functions appear in elastic processes so their corresponding Winger d-functions have $\lambda_{12} = \lambda_{34} \equiv \lambda$.

We first consider $C_{s,u}(m,J), D_{s,u}(m,J)$ and $F_{s,u}(m,J)$, that can be written in a generic way as

$$\mathcal{S}^J_{\lambda,\lambda} = \int_0^{p_{\max}} dp\, 2p\, S(p)\, d^J_{\lambda,\lambda}(1-2p^2) \quad \text{with} \quad p = \sqrt{-t/m^2}\,. \tag{C.1}$$

Notice that in $S(p)$ we incorporate not only the smearing function but also possible powers of $m^2/(m^2+t) = 1/(1-p^2)$.

We begin by deriving a necessary condition for the positivity of Eq. (C.1) in the limit $J \to \infty$ at fixed m^2. As shown in Fig. 6, the Winger d-functions monotonically increases or decreases for $p > 1$, leading to $d^J_{\lambda,\lambda} \to (-1)^J \infty$ as $p \to \infty$, except for $d^0_{0,0} = 1$.[12] Furthermore, the divergence toward $\pm\infty$ becomes stronger as J increases; therefore, it cannot be tamed by any smearing function in the $J \to \infty$ limit. This forces us to impose $p_{\max} \leq 1$ in order to ensure that Eq. (C.1) remains positive as $J \to \infty$.[13]

Fig. 6 also shows that the Wigner d-functions with identical sub-indices are positive around $p \sim 0$ for all J, while oscillates as p approaches 1. Thus, the smearing function must be chosen to enhance the region $p \sim 0$ and suppress the oscillatory behavior. This can be achieved by setting the smearing function proportional to

$$S(p) \propto (1 - p/p_{\max})^r = (1 - \sqrt{-t/|t|_{\max}})^r \quad \text{with} \quad r \geq 0, \tag{C.2}$$

where $p/p_{\max}$ is introduced to prevent the smearing function from depending on m. In the main text, we set $r = 5$, which is sufficient to suppress oscillatory contributions. We note that although many alternatives of the smearing function could satisfy the positivity conditions discussed so far, they do not result in a significant difference in the final bound [27].

We can proceed in the same way for $B_{s,u}(m,J)$ in which the smearing is performed over w instead of t. In this case, a few remarks are in order. For $B_s(m,J)$ we observe that the Wigner d-function involved monotonically increases (decreases) for even (odd) $J/2 > 0$ in the region $w > m^2/4$.[14] Thus, we must require

$$w_{\max} \leq m^2/4 \quad \text{for } B_s(m,J), \tag{C.3}$$

to ensure positivity for all J. On the other hand, we find that for $B_u(m,J)$ one can always find a smearing function that guarantees positivity. This is because the argument of the Wigner d-

[12] We will deduce this limit in Eq. (C.6).

[13] $C_s(m,J)$ escapes this logic since only even J is allowed, and therefore its positive sign for $p \gg 1$ is fixed; with a proper smearing function, it can be made always positive.

[14] For $p = \sqrt{4w/m^2}$, we have $d^J_{0,0}(\sqrt{1-p^2}) \propto (-1)^{J/2}(p-1)$ near $p = 1$ for even $J > 0$.

function is $(m^2-w)/(m^2+w)$ that is always between 1 and -1 where the Wigner d-function does not diverge for any J.

C.1 Maximal $|t|_{\max}$ as a function of J

In the previous section, we have seen that a generic bound to have Eq. (C.1) positive for all J corresponds to $p_{\max}=\sqrt{|t|_{\max}/m^2}\leq 1$. This fixes $|t|_{\max}=\mathrm{Min}[M_s,M_u]$, where we recall that $M_{s,u}$ are the masses of the s- and u-channel lightest UV state.

Nevertheless, one can consider the possibility of taking larger values of $|t|_{\max}$, as this would lead to stronger bounds. We aim here to identify the largest J for which we can take $|t|_{\max}=M_J^2$ without losing positivity, where M_J denotes the mass of the lightest UV state with spin J. As shown in the main text, this will determine the spin of the states that must appear at the causal cutoff Λ_{caus}, providing crucial information about the UV completion.

The above goal requires a detail inspection of smearing each Wigner d-function as a function of J, starting from its lowest possible value. We obtain the following result. Taking $|t|_{\max}=M_J^2$, the values of J are

- $J\geq 2$ for $B_s\geq 0$,
- $J\geq 3$ for $B_u\geq 0, D_u\geq 0, F_u\geq 0$,
- $J\geq 4$ for $C_s\geq 0, D_s\geq 0, F_s\geq 0$,

with no restriction on J for satisfying $C_s\geq 0$. In the rest of the section, we provide a detailed explanation of the cases of $B_s(m,J)$ and $F_u(m,J)$, which determine the J values in Eq. (4.26) and Eq. (4.41), respectively. These are essential for interpreting the bounds Eq. (4.27) and Eq. (4.42). The remaining cases can be straightforwardly obtained by following the argument presented here.

$B_s(m,J)$ includes $d^J_{0,0}$ allowing, in principle, $J=0,2,4,\ldots$.[15] For $J=0$, $d^0_{0,0}$ is constant, so it is easy to guarantee the positivity of $B_s(m,0)$ for any $w_{\max}$. Next, we consider $d^2_{0,0}$. It decreases for $\omega_{\max}>m^2/4$, requiring then to take $w_{\max}=M^2_{J=2}/4$, or equivalently, $|t|_{\max}=M^2_{J=2}$ to have $B_s(m,2)\geq 0$. The UV state of mass $M_{J=2}$ couples to $\gamma^+\gamma^+$ and h^-h^-.

For $F_u(m,J)$ (with the same structure as $D_u(m,J)$), involving $d^J_{1,1}/(m^2+t)$, we can have $J=1,2,3,\ldots$. The proportionality,

$$d^J_{\lambda,\lambda}(1-2p^2)\propto(1-p^2)^{|\lambda|}P^{(0,|\lambda|)}_{J-|\lambda|}(1-2p^2), \tag{C.4}$$

with $P^{(\alpha,\beta)}_n$ the Jacobi polynomial, guarantees that $d^1_{1,1}/(m^2+t)$ is constant, and $F_u(m,1)\geq 0$ for any $|t|_{\max}$. On the other hand, $d^2_{1,1}/(m^2+t)$ decreases monotonically to negative values for $|t|>m^2$. In spite of this, by taking the smearing function to involve a Bessel function, we can cancel the negative contribution and obtain $F_u(m,2)\geq 0$. In contrast, the Bessel function cancels

[15] Recall that $B_s(m,J)$ arise from the s-channel of $\gamma^+\gamma^+\to\gamma^+\gamma^+$, restricting J to even values.

the positive contribution of $d^3_{1,1}/(m^2+t)$ for $|t|>m^2$, determining that $|t|_{\rm max}$ cannot be larger than $M^2_{J=3}$ in order to have $F_u(m^2,3)\geq 0$. The UV state of mass $M_{J=3}$ couples to γ^+h^+ and γ^-h^+.

C.2 High-J asymptotics of the smeared Wigner d-functions

To confirm the positivity of $B_{s,u}(m,J)$, $C_{s,u}(m,J)$, $D_{s,u}(m,J)$ and $F_{s,u}(m,J)$, and also the validity of Eqs. (4.16) and (4.34) for all J, we must understand the high-J asymptotics of the smeared Wigner d-functions as numerical evaluation cannot access the $J\to\infty$ limit.

We first consider the aymptotics of $S^J_{\lambda,\lambda'}$ with different sub-indices from Eq. (C.1) for any $p_{\rm max}\leq 1$, applicable to the smeared Wigner d-functions with the variable t. For the lower $p_{\rm max}<1$, the smearing function with $(1-p/p_{\rm max})^r$ suppresses the oscillatory contributions more strongly.

Therefore, it suffices to evaluate the asymptotics of $S^J_{\lambda,\lambda'}$ only at $p_{\rm max}=1$, leading to our target:

$$\mathcal{A}_{\lambda,\lambda'}(J)\equiv\lim_{J\to\infty}\mathcal{S}^J_{\lambda,\lambda'}=\lim_{J\to\infty}\int_0^\pi\frac{\sin\theta d\theta}{2}S(\sin\tfrac{\theta}{2})d^J_{\lambda,\lambda'}(\cos\theta),\tag{C.5}$$

where we have changed variables, $\cos\theta\equiv 1-2p^2$. In the high-J limit, the Wigner d-function becomes rapidly oscillatory, but the stationary phase method [94,95] shows that bulk contributions cancel while the endpoint contributions remain. This allows us to use the asymptotic expressions of the Wigner d-function instead of the exact form:[16]

$$d^J_{\lambda,\lambda'}(\theta)\sim\begin{cases}(-1)^{\frac{\lambda_-+|\lambda_-|}{2}}J_{|\lambda_-|}(J\theta) & \text{for }\theta\ll 1,\\ (-1)^{\frac{-|\lambda_-|+|\lambda_+|-2J}{2}}J_{|\lambda_+|}\big[J(\pi-\theta)\big] & \text{for }\pi-\theta\ll 1\end{cases},\tag{C.6}$$

at $J\gg 1$ where $\lambda_\pm=\lambda\pm\lambda'$ and J_λ is the Bessel function of the first kind. This is because the two asymptotics match the Wigner d-function at the endpoints, $\theta=0$ and π, respectively, while their magnitude is suppressed as $1/\sqrt{J}$ in the bulk, enabling us to rewrite Eq. (C.5) as

$$\begin{aligned}\mathcal{A}_{\lambda,\lambda'}(J)=\lim_{J\to\infty}\Big\{&(-1)^{\frac{\lambda_-+|\lambda_-|}{2}}\int_0^a\frac{\sin\theta d\theta}{2}S(\sin\tfrac{\theta}{2})J_{|\lambda_-|}(J\theta)\\ &+(-1)^{\frac{-|\lambda_-|+|\lambda_+|-2J}{2}}\int_b^\pi\frac{\sin\theta d\theta}{2}S(\sin\tfrac{\theta}{2})J_{|\lambda_+|}\big[J(\pi-\theta)\big]\Big\},\end{aligned}\tag{C.7}$$

in terms of arbitrarily finite cutoffs, $a>0$ and $b<\pi$.

Due to the endpoint dominance, we can use the Taylor expansion of the smearing function with the sine factor near the endpoints. The smearing function that we consider is

$$S(\sin\tfrac{\theta}{2})\equiv(\sin\tfrac{\theta}{2})^\alpha\widetilde{S}(\sin\tfrac{\theta}{2})\quad\text{with}\quad 0\leq\alpha<1,\tag{C.8}$$

[16] In this work, we adopt the convention of the d-function in Ref. [96].

which is non-analytic at $\theta = 0$ for $\alpha > 0$. Expanding this as

$$\frac{\sin\theta}{2} S(\sin\tfrac{\theta}{2}) = \frac{\theta^\alpha}{2^{1+\alpha}} \left[\theta \widetilde{S}(0) + \frac{\theta^2}{2}\widetilde{S}'(0) + \cdots\right] \qquad \text{for } \theta \ll 1, \tag{C.9}$$

$$\frac{\sin\theta}{2} S(\sin\tfrac{\theta}{2}) = \frac{1}{2} \left[\theta \widetilde{S}(1) - \frac{\theta^2}{24}\left[(4+3\alpha)\widetilde{S}(1) + \widetilde{S}'(1)\right] + \cdots\right] \qquad \text{for } \pi - \theta \ll 1, \tag{C.10}$$

at each endpoint, we can get the asymptotics by putting the expansions above into Eq. (C.7):

$$\begin{aligned}\mathcal{A}_{\lambda,\lambda'}(J) = (-1)^{\frac{\lambda_- + |\lambda_-|}{2}} &\left\{ \frac{\Gamma[(2+|\lambda_-|+\alpha)/2]}{J^{2+\alpha}\Gamma[(|\lambda_-|-\alpha)/2]} \widetilde{S}^{(0)}(0) + \frac{\Gamma[(3+|\lambda_-|+\alpha)/2]}{J^{3+\alpha}\Gamma[(|\lambda_-|-1-\alpha)/2]} \widetilde{S}^{(1)}(0) + \cdots \right\} \\ + (-1)^{\frac{-\lambda_- + |\lambda_+| - 2J}{2}} &\left\{ \frac{|\lambda_+|}{2J^2} \widetilde{S}^{(0)}(1) - \frac{|\lambda_+|(|\lambda_+|^2 - 4)}{48 J^4} \left[(4+3\alpha)\widetilde{S}^{(0)}(1) + 3\widetilde{S}^{(1)}(1)\right] + \cdots \right\},\end{aligned} \tag{C.11}$$

Here, we used the analytic integral,

$$\lim_{J\to\infty} \int_0^a \theta^{1+n} J_\lambda(J\theta)\, d\theta = \frac{2^{1+n}\Gamma\left(1 + \frac{\lambda+n}{2}\right)}{J^{2+n}\Gamma\left(\frac{\lambda-n}{2}\right)} + a\text{-dependent oscillatory terms}, \tag{C.12}$$

where we neglected the oscillatory terms, ensured by the stationary phase method.

Similarly to the case of smeared Wigner d-functions with the variable t, we can derive the asymptotics of those with the variable w. Taking the critical case $w_{\rm max} = m^2/4$ in Eq. (C.3), the asymptotics involving $d^J_{\lambda,\lambda}(\sqrt{1 - 4w/m^2})$ can be given by

$$\int_0^{\pi/2} \sin 2\theta\, d\theta\, S(\sin\theta)\, d^J_{\lambda,\lambda}(\cos\theta), \tag{C.13}$$

where we use $\sqrt{1 - 4w/m^2} = \cos\theta$. Note that the integration region is restricted to $\pi/2$, allowing only the endpoint $\theta = 0$ contribution to be dominant due to the $1/\sqrt{J}$ supression of the Winger d-function at bulk.

As mentioned before, the argument $(m^2 - w)/(m^2 + w)$ of the Wigner d-function is put only between -1 and 1, allowing to make always the relevant smeared ones positive via a suitable choice of the smearing function. However, as shown in Eq. (C.3), our choice making $B_s(m, J)$ positive for $w_{\rm max} \leq m^2/4$ leads $B_u(m, J)$ to be negative for a specific J value. It is easy to see where the negativity arise from by writing the smeared one as

$$\int_0^{\Theta_{\rm max}} \frac{2\sin\theta\, d\theta}{(1+\cos\theta)^2} S\left(\frac{1-\cos\theta}{\sin\theta}\right) d^J_{\lambda,\lambda}(\cos\theta), \tag{C.14}$$

where we use $(m^2 - w)/(m^2 + w) = \cos\theta$ with $\Theta_{\rm max} = \cos^{-1}[(m^2 - w_{\rm max})/(m^2 + w_{\rm max})]$. For the function S adopting the smearing function in Eq. (4.24) is proportional to

$$S\left(\frac{1-\cos\theta}{\sin\theta}\right) \propto 4\left(1-\frac{1-\cos\theta}{\Delta_{\max}\sin\theta}\right)^5 \quad \text{with} \quad \Delta_{\max}=\frac{1-\cos\Theta_{\max}}{\sin\Theta_{\max}}, \tag{C.15}$$

which vanishes at $\theta = \Theta_{\max}$. This function cannot cancels the monotonic growth of the factor $\sin\theta/(1+\cos\theta)^2$ for $\theta \to \pi$ and moreover, the extra factor $(m^2+2w)(m^2+w)^{k-1}$ is replaced to involve an additional power of $1/(1+\cos\theta)$ in the integral in Eq. (C.14). Since $d^J_{\lambda,\lambda}$ is oscillatory near $\theta = \pi$, it leads us to lose the positivity for all J.

References

[1] M. Kruczenski, J. Penedones, and B. C. van Rees, "Snowmass White Paper: S-matrix Bootstrap," arXiv:2203.02421 [hep-th].

[2] M. F. Paulos, J. Penedones, J. Toledo, B. C. van Rees, and P. Vieira, "The S-matrix bootstrap II: two dimensional amplitudes," *JHEP* **11** (2017) 143, arXiv:1607.06110 [hep-th].

[3] M. F. Paulos, J. Penedones, J. Toledo, B. C. van Rees, and P. Vieira, "The S-matrix bootstrap. Part III: higher dimensional amplitudes," *JHEP* **12** (2019) 040, arXiv:1708.06765 [hep-th].

[4] A. L. Guerrieri, J. Penedones, and P. Vieira, "Bootstrapping QCD Using Pion Scattering Amplitudes," *Phys. Rev. Lett.* **122** no. 24, (2019) 241604, arXiv:1810.12849 [hep-th].

[5] N. Doroud and J. Elias Miró, "S-matrix bootstrap for resonances," *JHEP* **09** (2018) 052, arXiv:1804.04376 [hep-th].

[6] C. de Rham, S. Melville, A. J. Tolley, and S.-Y. Zhou, "Positivity Bounds for Massive Spin-1 and Spin-2 Fields," *JHEP* **03** (2019) 182, arXiv:1804.10624 [hep-th].

[7] C. Zhang and S.-Y. Zhou, "Positivity bounds on vector boson scattering at the LHC," *Phys. Rev. D* **100** no. 9, (2019) 095003, arXiv:1808.00010 [hep-ph].

[8] B. Bellazzini, F. Riva, J. Serra, and F. Sgarlata, "Massive Higher Spins: Effective Theory and Consistency," *JHEP* **10** (2019) 189, arXiv:1903.08664 [hep-th].

[9] G. N. Remmen and N. L. Rodd, "Consistency of the Standard Model Effective Field Theory," *JHEP* **12** (2019) 032, arXiv:1908.09845 [hep-ph].

[10] B. Bellazzini, M. Lewandowski, and J. Serra, "Positivity of Amplitudes, Weak Gravity Conjecture, and Modified Gravity," *Phys. Rev. Lett.* **123** no. 25, (2019) 251103, arXiv:1902.03250 [hep-th].

[11] Y.-t. Huang, J.-Y. Liu, L. Rodina, and Y. Wang, "Carving out the Space of Open-String S-matrix," *JHEP* **04** (2021) 195, `arXiv:2008.02293 [hep-th]`.

[12] A. Sinha and A. Zahed, "Crossing Symmetric Dispersion Relations in Quantum Field Theories," *Phys. Rev. Lett.* **126** no. 18, (2021) 181601, `arXiv:2012.04877 [hep-th]`.

[13] B. Bellazzini, J. Elias Miró, R. Rattazzi, M. Riembau, and F. Riva, "Positive moments for scattering amplitudes," *Phys. Rev. D* **104** no. 3, (2021) 036006, `arXiv:2011.00037 [hep-th]`.

[14] A. J. Tolley, Z.-Y. Wang, and S.-Y. Zhou, "New positivity bounds from full crossing symmetry," *JHEP* **05** (2021) 255, `arXiv:2011.02400 [hep-th]`.

[15] A. Hebbar, D. Karateev, and J. Penedones, "Spinning S-matrix bootstrap in 4d," *JHEP* **01** (2022) 060, `arXiv:2011.11708 [hep-th]`.

[16] N. Arkani-Hamed, T.-C. Huang, and Y.-t. Huang, "The EFT-Hedron," *JHEP* **05** (2021) 259, `arXiv:2012.15849 [hep-th]`.

[17] S. Caron-Huot and V. Van Duong, "Extremal Effective Field Theories," *JHEP* **05** (2021) 280, `arXiv:2011.02957 [hep-th]`.

[18] S. Caron-Huot, D. Mazac, L. Rastelli, and D. Simmons-Duffin, "Sharp boundaries for the swampland," *JHEP* **07** (2021) 110, `arXiv:2102.08951 [hep-th]`.

[19] Z. Bern, D. Kosmopoulos, and A. Zhiboedov, "Gravitational effective field theory islands, low-spin dominance, and the four-graviton amplitude," *J. Phys. A* **54** no. 34, (2021) 344002, `arXiv:2103.12728 [hep-th]`.

[20] L.-Y. Chiang, Y.-t. Huang, W. Li, L. Rodina, and H.-C. Weng, "Into the EFThedron and UV constraints from IR consistency," *JHEP* **03** (2022) 063, `arXiv:2105.02862 [hep-th]`.

[21] J. Henriksson, B. McPeak, F. Russo, and A. Vichi, "Rigorous bounds on light-by-light scattering," *JHEP* **06** (2022) 158, `arXiv:2107.13009 [hep-th]`.

[22] A. Zahed, "Positivity and geometric function theory constraints on pion scattering," *JHEP* **12** (2021) 036, `arXiv:2108.10355 [hep-th]`.

[23] B. Alvarez, J. Bijnens, and M. Sjö, "NNLO positivity bounds on chiral perturbation theory for a general number of flavours," *JHEP* **2022** (2022) 159, `arXiv:2112.04253 [hep-ph]`.

[24] J. Elias Miro, A. Guerrieri, and M. A. Gumus, "Bridging positivity and S-matrix bootstrap bounds," *JHEP* **05** (2023) 001, `arXiv:2210.01502 [hep-th]`.

[25] F. Serra, J. Serra, E. Trincherini, and L. G. Trombetta, "Causality constraints on black holes beyond GR," *JHEP* **08** (2022) 157, `arXiv:2205.08551 [hep-th]`.

[26] S. Caron-Huot, Y.-Z. Li, J. Parra-Martinez, and D. Simmons-Duffin, "Causality constraints on corrections to Einstein gravity," *JHEP* **05** (2023) 122, arXiv:2201.06602 [hep-th].

[27] S. Caron-Huot, Y.-Z. Li, J. Parra-Martinez, and D. Simmons-Duffin, "Graviton partial waves and causality in higher dimensions," *Phys. Rev. D* **108** no. 2, (2023) 026007, arXiv:2205.01495 [hep-th].

[28] J. Henriksson, B. McPeak, F. Russo, and A. Vichi, "Bounding violations of the weak gravity conjecture," *JHEP* **08** (2022) 184, arXiv:2203.08164 [hep-th].

[29] J. Albert and L. Rastelli, "Bootstrapping pions at large N," *JHEP* **08** (2022) 151, arXiv:2203.11950 [hep-th].

[30] C. Fernandez, A. Pomarol, F. Riva, and F. Sciotti, "Cornering large-N_c QCD with positivity bounds," *JHEP* **06** (2023) 094, arXiv:2211.12488 [hep-th].

[31] F. Acanfora, A. Guerrieri, K. Häring, and D. Karateev, "Bounds on scattering of neutral Goldstones," *JHEP* **03** (2024) 028, arXiv:2310.06027 [hep-th].

[32] Y. He and M. Kruczenski, "Bootstrapping gauge theories," *Phys. Rev. Lett.* **133** (2024) 191601, arXiv:2309.12402 [hep-th].

[33] A. L. Guerrieri, A. Hebbar, and B. C. van Rees, "Constraining Glueball Couplings," arXiv:2312.00127 [hep-th].

[34] J. Albert and L. Rastelli, "Bootstrapping pions at large N. Part II. Background gauge fields and the chiral anomaly," *JHEP* **09** (2024) 039, arXiv:2307.01246 [hep-th].

[35] T. Ma, A. Pomarol, and F. Sciotti, "Bootstrapping the chiral anomaly at large N_c," *JHEP* **11** (2023) 176, arXiv:2307.04729 [hep-th].

[36] B. Bellazzini, G. Isabella, S. Ricossa, and F. Riva, "Massive gravity is not positive," *Phys. Rev. D* **109** no. 2, (2024) 024051, arXiv:2304.02550 [hep-th].

[37] Y.-Z. Li, "Effective field theory bootstrap, large-N χPT and holographic QCD," *JHEP* **01** (2024) 072, arXiv:2310.09698 [hep-th].

[38] J. Albert, J. Henriksson, L. Rastelli, and A. Vichi, "Bootstrapping mesons at large N: Regge trajectory from spin-two maximization," *JHEP* **09** (2024) 172, arXiv:2312.15013 [hep-th].

[39] D.-Y. Hong, Z.-H. Wang, and S.-Y. Zhou, "Causality bounds on scalar-tensor EFTs," *JHEP* **10** (2023) 135, arXiv:2304.01259 [hep-th].

[40] Y. He and M. Kruczenski, "Gauge Theory Bootstrap: Pion amplitudes and low energy parameters," arXiv:2403.10772 [hep-th].

[41] A. Guerrieri, K. Häring, and N. Su, "From data to the analytic S-matrix: A Bootstrap fit of the pion scattering amplitude," arXiv:2410.23333 [hep-th].

[42] C. Beadle, G. Isabella, D. Perrone, S. Ricossa, F. Riva, and F. Serra, "Non-forward UV/IR relations," *JHEP* **08** (2025) 188, arXiv:2407.02346 [hep-th].

[43] F. Bertucci, J. Henriksson, B. McPeak, S. Ricossa, F. Riva, and A. Vichi, "Positivity bounds on massive vectors," *JHEP* **12** (2024) 051, arXiv:2402.13327 [hep-th].

[44] J. Albert, W. Knop, and L. Rastelli, "Where is tree-level string theory?," *JHEP* **02** (2025) 157, arXiv:2406.12959 [hep-th].

[45] H. Xu, D.-Y. Hong, Z.-H. Wang, and S.-Y. Zhou, "Positivity bounds on parity-violating scalar-tensor EFTs," *JCAP* **01** (2025) 102, arXiv:2410.09794 [hep-th].

[46] J. Berman, "Analytic bounds on the spectrum of crossing symmetric S-matrices," *JHEP* **08** (2025) 066, arXiv:2410.01914 [hep-th].

[47] K. Häring and A. Zhiboedov, "What is the graviton pole made of?," arXiv:2410.21499 [hep-th].

[48] Z.-Y. Dong, T. Ma, A. Pomarol, and F. Sciotti, "Bootstrapping the chiral-gravitational anomaly," *JHEP* **05** (2025) 114, arXiv:2411.14422 [hep-th].

[49] C. Beadle, G. Isabella, D. Perrone, S. Ricossa, F. Riva, and F. Serra, "The EFT bootstrap at finite M_{PL}," *JHEP* **06** (2025) 209, arXiv:2501.18465 [hep-th].

[50] C.-H. Chang and J. Parra-Martinez, "Graviton loops and negativity," *JHEP* **08** (2025) 175, arXiv:2501.17949 [hep-th].

[51] C. Pasiecznik, "Bootstrapping Gravity with Crossing Symmetric Dispersion Relations," arXiv:2506.09884 [hep-th].

[52] Y.-t. Huang, S. Ricossa, F. Riva, and J.-D. Tsai, "The Rise of Linear Trajectories," arXiv:2510.07991 [hep-th].

[53] X. O. Camanho, J. D. Edelstein, J. Maldacena, and A. Zhiboedov, "Causality Constraints on Corrections to the Graviton Three-Point Coupling," *JHEP* **02** (2016) 020, arXiv:1407.5597 [hep-th].

[54] O. Aharony, S. S. Gubser, J. M. Maldacena, H. Ooguri, and Y. Oz, "Large N field theories, string theory and gravity," *Phys. Rept.* **323** (2000) 183–386, arXiv:hep-th/9905111.

[55] S. Cremonini, K. Hanaki, J. T. Liu, and P. Szepietowski, "Higher derivative effects on eta/s at finite chemical potential," *Phys. Rev. D* **80** (2009) 025002, arXiv:0903.3244 [hep-th].

[56] T. Delsate, V. Cardoso, and P. Pani, "Anti de Sitter black holes and branes in dynamical Chern-Simons gravity: perturbations, stability and the hydrodynamic modes," *JHEP* **06** (2011) 055, `arXiv:1103.5756 [hep-th]`.

[57] S. R. Das, S. Giusto, S. D. Mathur, Y. Srivastava, X. Wu, and C. Zhou, "Branes wrapping black holes," *Nucl. Phys. B* **733** (2006) 297–333, `arXiv:hep-th/0507080`.

[58] A. Donos and J. P. Gauntlett, "Black holes dual to helical current phases," *Phys. Rev. D* **86** (2012) 064010, `arXiv:1204.1734 [hep-th]`.

[59] R.-G. Cai, T.-J. Li, Y.-H. Qi, and Y.-L. Zhang, "Incompressible Navier-Stokes Equations from Einstein Gravity with Chern-Simons Term," *Phys. Rev. D* **86** (2012) 086008, `arXiv:1208.0658 [hep-th]`.

[60] E. Megias and F. Pena-Benitez, "Holographic Gravitational Anomaly in First and Second Order Hydrodynamics," *JHEP* **05** (2013) 115, `arXiv:1304.5529 [hep-th]`.

[61] T. Azeyanagi, R. Loganayagam, and G. S. Ng, "Anomalies, Chern-Simons Terms and Black Hole Entropy," *JHEP* **09** (2015) 121, `arXiv:1505.02816 [hep-th]`.

[62] A. Bhattacharyya, L. Cheng, and L.-Y. Hung, "Relative Entropy, Mixed Gauge-Gravitational Anomaly and Causality," *JHEP* **07** (2016) 121, `arXiv:1605.02553 [hep-th]`.

[63] Y. Liu and F. Pena-Benitez, "Spatially modulated instabilities of holographic gauge-gravitational anomaly," *JHEP* **05** (2017) 111, `arXiv:1612.00470 [hep-th]`.

[64] M. Baggioli, Y. Bu, and X. Sun, "Chiral anomalous magnetohydrodynamics in action: effective field theory and holography," *JHEP* **04** (2025) 126, `arXiv:2412.02361 [hep-th]`.

[65] L. J. Dixon, "A brief introduction to modern amplitude methods," in *Theoretical Advanced Study Institute in Elementary Particle Physics: Particle Physics: The Higgs Boson and Beyond*, pp. 31–67. 2014. `arXiv:1310.5353 [hep-ph]`.

[66] B. Bellazzini, G. Isabella, M. Lewandowski, and F. Sgarlata, "Gravitational causality and the self-stress of photons," *JHEP* **05** (2022) 154, `arXiv:2108.05896 [hep-th]`.

[67] M. Jacob and G. C. Wick, "On the General Theory of Collisions for Particles with Spin," *Annals Phys.* **7** (1959) 404–428.

[68] M. Froissart, "Asymptotic behavior and subtractions in the mandelstam representation," *Phys. Rev.* **123** (1961) 1053–1057.

[69] A. Martin, "Extension of the axiomatic analyticity domain of scattering amplitudes by unitarity. 1.," *Nuovo Cim. A* **42** (1965) 930–953.

[70] J. Kaplan and S. Kundu, “A Species or Weak-Gravity Bound for Large N Gauge Theories Coupled to Gravity,” *JHEP* **11** (2019) 142, arXiv:1904.09294 [hep-th].

[71] J. Kaplan and S. Kundu, “Closed Strings and Weak Gravity from Higher-Spin Causality,” *JHEP* **02** (2021) 145, arXiv:2008.05477 [hep-th].

[72] J. Kaplan and S. Kundu, “Causality constraints in large N QCD coupled to gravity,” *Phys. Rev. D* **104** no. 6, (2021) L061901, arXiv:2009.08460 [hep-th].

[73] N. Afkhami-Jeddi, S. Kundu, and A. Tajdini, “A Bound on Massive Higher Spin Particles,” *JHEP* **04** (2019) 056, arXiv:1811.01952 [hep-th].

[74] E. Witten, “Current Algebra Theorems for the U(1) Goldstone Boson,” *Nucl. Phys. B* **156** (1979) 269–283.

[75] G. Veneziano, “U(1) Without Instantons,” *Nucl. Phys. B* **159** (1979) 213–224.

[76] G. ’t Hooft, “A Planar Diagram Theory for Strong Interactions,” *Nucl. Phys. B* **72** (1974) 461.

[77] E. Witten, “Baryons in the 1/n Expansion,” *Nucl. Phys. B* **160** (1979) 57–115.

[78] W. Israel, “Singular hypersurfaces and thin shells in general relativity,” *Nuovo Cim. B* **44S10** (1966) 1. [Erratum: Nuovo Cim.B 48, 463 (1967)].

[79] R. Barbieri, A. Pomarol, and R. Rattazzi, “Weakly coupled Higgsless theories and precision electroweak tests,” *Phys. Lett. B* **591** (2004) 141–149, arXiv:hep-ph/0310285.

[80] A. Manohar and H. Georgi, “Chiral Quarks and the Nonrelativistic Quark Model,” *Nucl. Phys. B* **234** (1984) 189–212.

[81] L. Randall and R. Sundrum, “A Large mass hierarchy from a small extra dimension,” *Phys. Rev. Lett.* **83** (1999) 3370–3373, arXiv:hep-ph/9905221.

[82] N. Arkani-Hamed, M. Porrati, and L. Randall, “Holography and phenomenology,” *JHEP* **08** (2001) 017, arXiv:hep-th/0012148.

[83] M. Kruczenski, D. Mateos, R. C. Myers, and D. J. Winters, “Meson spectroscopy in AdS / CFT with flavor,” *JHEP* **07** (2003) 049, arXiv:hep-th/0304032.

[84] N. Afkhami-Jeddi, S. Kundu, and A. Tajdini, “A Conformal Collider for Holographic CFTs,” *JHEP* **10** (2018) 156, arXiv:1805.07393 [hep-th].

[85] I. H. Stairs, S. E. Thorsett, J. H. Taylor, and A. Wolszczan, “Studies of the relativistic binary pulsar psr b1534+12: I. timing analysis,” *Astrophys. J.* **581** (2002) 501–508, arXiv:astro-ph/0208357.

[86] I. H. Stairs, D. J. Nice, S. E. Thorsett, and J. H. Taylor, "Recent arecibo timing of the relativistic binary PSR B1534+12," in *34th Rencontres de Moriond: Gravitational Waves and Experimental Gravity*, pp. 309–318. 3, 1999. `arXiv:astro-ph/9903289`.

[87] A. R. Prasanna and S. Mohanty, "Constraints on nonminimally coupled curved space electrodynamics from astrophysical observations," *Class. Quant. Grav.* **20** (2003) 3023–3028, `arXiv:gr-qc/0306021`.

[88] X.-F. Wu, J.-J. Wei, M.-X. Lan, H. Gao, Z.-G. Dai, and P. Mészáros, "New test of weak equivalence principle using polarized light from astrophysical events," *Phys. Rev. D* **95** no. 10, (2017) 103004, `arXiv:1703.09935 [astro-ph.HE]`.

[89] S. Jana and S. Shankaranarayanan, "Non-Minimally Coupled Electromagnetic Fields and Observable Implications for Primordial Black Holes," *Universe* **10** no. 7, (2024) 270, `arXiv:2110.06056 [gr-qc]`.

[90] R. Carballo-Rubio, H. Delaporte, A. Eichhorn, and P. G. S. Fernandes, "Non-minimal light-curvature couplings and black-hole imaging," `arXiv:2505.21431 [astro-ph.HE]`.

[91] Y. Chen, Y. Liu, R.-S. Lu, Y. Mizuno, J. Shu, X. Xue, Q. Yuan, and Y. Zhao, "Stringent axion constraints with Event Horizon Telescope polarimetric measurements of M87," *Nature Astron.* **6** no. 5, (2022) 592–598, `arXiv:2105.04572 [hep-ph]`.

[92] J. Elias Miró, A. Guerrieri, M. A. Gümüs, and A. Zahed, "A Geometric View on Crossing-Symmetric Dispersion Relations," `arXiv:2509.14170 [hep-th]`.

[93] B. Bellazzini, A. Pomarol, M. Romano, and F. Sciotti, "(Super) Gravity from Positivity," `arXiv:2507.12535 [hep-th]`.

[94] N. Bleistein and R. A. Handelsman, *Asymptotic Expansions of Integrals*. Dover Publications, 1986.

[95] E. M. Stein and R. Shakarchi, *Real Analysis: Measure Theory, Integration, and Hilbert Spaces*. Princeton Lectures in Analysis, Volume 3. Princeton University Press, 2005.

[96] M. E. Rose, *Elementary Theory of Angular Momentum*. Dover Publications, New York, dover ed. ed., 1995.